European Journal of Medicinal Chemistry 297 (2025) 117965

Contents lists available at ScienceDirect

European Journal of Medicinal Chemistry

journal homepage: www.elsevier.com/locate/ejmech

Research paper

Targeting $\alpha_4\beta_1$ integrin: from cyclic to linear ligands, effects of chemical modifications

Valentina Giraldi [a,1], Andrea Maurizio [b,1], Martina Cirillo [a], Paolo Magnone [a], Emanuela Fedele [a], Andrea Bedini [b], Monica Baiula [b,*], Daria Giacomini [a,**]

[a] Department of Chemistry "Giacomo Ciamician" University of Bologna, Via Piero Gobetti, 85, 40129, Bologna, Italy
[b] Department of Pharmacy and Biotechnology, University of Bologna, Via Irnerio, 48, 40126, Bologna, Italy

ARTICLE INFO

Keywords:
Integrins
Agonists
Antagonists
Leukocytes
Inflammation
Lactams
Intracellular signalling

ABSTRACT

The immune system depends on integrins for adhesion and migration during leukocyte trafficking and for intracellular signalling. There is a causal relationship between dysregulation of integrin expression and the onset of pathological conditions, such as autoimmune diseases, inflammation, cancer, and infections. Therefore, integrins, such as $\alpha_4\beta_1$, are considered important therapeutic targets. In this study, a series of novel compounds were synthesized and evaluated for affinity and potency towards $\alpha_4\beta_1$, and selectivity towards $\alpha_5\beta_1$, and $\alpha_M\beta_2$ integrins. Three compounds **3**, **4**, and **8** showed excellent binding affinities ($K_i < 10$ nM) for $\alpha_4\beta_1$. In cell adhesion assays these three ligands behaved as antagonists of $\alpha_4\beta_1$, as confirmed by integrin-mediated intracellular signalling with a functional selectivity over ERK1/2 signalling pathway. Notably, compound **4**, a proline derivative, was an antagonist against $\alpha_4\beta_1$ (IC_{50} 15 ± 3 nM) and an agonist against $\alpha_M\beta_2$ integrin (EC_{50} 23 ± 5 nM). Compound **2**, a fluorinated β-lactam derivative, was a selective and potent agonist of $\alpha_5\beta_1$ (EC_{50} 45.98 ± 7.92 nM). Compound **5**, although it seems to bind to a different site compared to LDV in $\alpha_4\beta_1$ integrin, showed an agonist behaviour in cell adhesion mediated by $\alpha_4\beta_1$ and $\alpha_5\beta_1$ integrin (EC_{50} 25 ± 3 and 4.8 ± 3.4 nM, respectively) and in activating $\alpha_4\beta_1$ integrin-mediated ERK1/2 and Akt phosphorylation. Compound **8** was the most potent agonist of the series against $\alpha_M\beta_2$ (EC_{50} 1.4 ± 0.2 nM). Overall, the present study provides new insights into the effects of new integrin ligands that could be considered as potential lead compounds for therapeutic applications in inflammatory diseases and cancer.

1. Introduction

Integrins are essential receptors that control interactions between cells and their surroundings by transmitting mechanical and biochemical signals [1–3]. Integrins are important for several cell signalling pathways that control fundamental processes such as survival, proliferation, differentiation, and migration [4].

As heterodimeric proteins composed by α and β subunits, 24 types of integrins are present on the surface of mammalian cells. There is evidence that each heterodimer could induce specific responses causing each cell type to respond differently to its surroundings [5]. Upon binding specific ligands, integrins are able to activate outside-in or inside-out signalling pathways by changing their conformational state in the ectodomain from an inactive to an active state [6–9]. Therefore, integrins could be defined not only by the composition of α or β subunits but also by interaction with specific ligands and specific cell-type expression [10,11].

The immune system depends on integrins for migration and adhesion during leukocyte trafficking and for intracellular signalling [4,12–15]. Integrins $\alpha_L\beta_2$, $\alpha_M\beta_2$, $\alpha_X\beta_2$, and $\alpha_D\beta_2$, are exclusively found on leukocytes and therefore are particularly important for the immune system. Neutrophils, for instance, require $\alpha_L\beta_2$ and $\alpha_M\beta_2$ for extravasation and migration during inflammation [16–19]. Integrin $\alpha_4\beta_1$ is expressed in many types of cells, stem and progenitor cells, T and B cells, monocytes, NK cells, and eosinophils [20]. Other integrins present on leukocytes are the two β_7 integrins $\alpha_4\beta_7$ and $\alpha_E\beta_7$, and also $\alpha_5\beta_1$, $\alpha_9\beta_1$, and $\alpha_v\beta_3$.

Integrins in immune cells are mainly involved in three processes: immune cell recruitment, cell-cell interactions, and modulation of

* Corresponding author. Department of Pharmacy and Biotechnology, University of Bologna, 40126 Bologna, Italy
** Corresponding author. Department of Chemistry "G. Ciamician", University of Bologna, 40129 Bologna, Italy
E-mail addresses: monica.baiula@unibo.it (M. Baiula), daria.giacomini@unibo.it (D. Giacomini).
[1] Contributed equally.

https://doi.org/10.1016/j.ejmech.2025.117965
Received 7 April 2025; Received in revised form 8 July 2025; Accepted 9 July 2025
Available online 10 July 2025

intracellular signal transduction. Several studies have stressed the importance of a causal relationship between dysregulation of integrin expression and functions, and the onset of pathological conditions, such as autoimmune diseases, inflammation, cancer, and infections [20–25]. In particular, $\alpha_4\beta_1$ is fundamental to leukocyte homing, trafficking, differentiation, activation, and survival; moreover, it is involved in the inflammatory reaction, inflammatory-based diseases, cancer progression, and metastasis [26,27]. Therefore, integrins, such as $\alpha_4\beta_1$, are considered therapeutic targets and some new molecules are under development for the treatment of integrin-mediated diseases [28,29].

The classical role of integrins as cell adhesion receptors is activated on binding suitable ligands in the ectodomain, in particular on recognizing small peptide sequences present on the extracellular matrix, cell surface receptors, or serum components [30–33]. Understanding the binding specificity of leukocyte integrins is important to determine the range of ligands that interact with these receptors. Target sequences in natural ligands of some leukocyte integrins are the tripeptide motives Arg-Gly-Asp (RGD), Leu-Asp-Val (LDV), or Leu-Asp-Thr (LDT) (Fig. 1) [34,35]. Upon this evidence, several molecules have been developed containing those tripeptides, but, moreover, other non-peptide ligands for leukocyte integrins were successfully obtained [36–38]. In particular, a recent advance in the therapeutic application of integrin ligands [39,40] has been the approval for human administration of Carotegrast, an orally active (Carotegrast methyl) antagonist of $\alpha_4\beta_1/\alpha_4\beta_7$ for the therapy of moderate ulcerative colitis [41].

Given the involvement of integrins in the regulation of multiple physiological processes [4], it would be highly desirable to have integrin subtype-selective molecules able to activate or deactivate specific integrins to get a more specific action, to limit undesirable side-effects, and to move forward more personalized pharmacological therapies.

Our interdisciplinary research group has been involved for some years in the search for new selective integrin ligands able to activate (agonist) or block (antagonist) specific integrins [42,43].

Among others, some molecules were found to have a high specific potency for leukocyte integrins (see Fig. 1). The new ligands are able to differently modulate cell signalling pathways: some compounds are agonists promoting cell adhesion and intracellular signalling activation, while others are antagonists inhibiting integrin-dependent cell functions.

Interestingly, several studies have suggested that small molecules that act as leukocyte integrin agonists may have therapeutic efficacy. These include an agonist of $\alpha_M\beta_2$ integrin that reprograms immunosuppressive myeloid cell responses, an agonist of $\alpha_L\beta_2$ integrin that inhibits lymphocyte *trans*-endothelial migration, and an agonist of $\alpha_4\beta_1$ integrin that induces progenitor cell adhesion and reprograms innate immunity to sensitize pancreatic cancer to immunotherapies [44,45].

A β-lactam-based small molecule **A** (Fig. 1) developed in our group as selective and potent agonist of $\alpha_4\beta_1$ integrin, found applications in promoting human mesenchymal stem cell (MSC) adhesion [46], as well as differentiation toward osteoblastic lineage in co-cultures of human primary mesenchymal stem cells (hMSCs) and human primary osteoclasts (OCs) [47]. It has also been successfully combined with poly (L-lactic acid) (PLLA) nanofibers to provide a controlled release of this agonist, resulting in a medication particularly suited to chronic skin wound healing [48].

Despite the selective binding and valuable potency of some of the previously studied molecules, it is relevant to recognize those structural requirements to address the selectivity and the agonist/antagonist

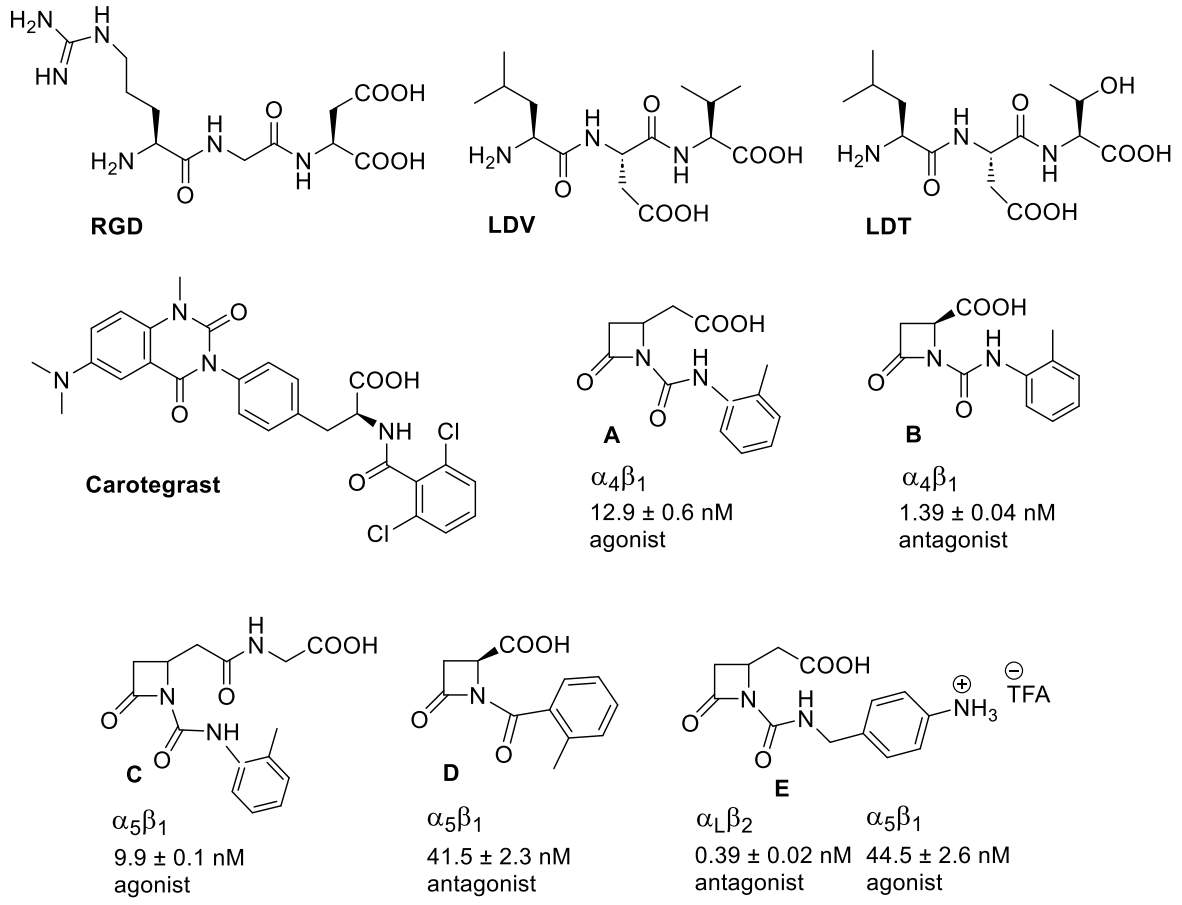

Fig. 1. Tripeptide sequences recognized by leukocyte integrins in natural ligands (RGD, LDV, and LDT) and Carotegrast, as approved drug; β-lactam compounds previously reported as selective integrin ligands (A–E, refs. 42, 43).

behaviour of new integrin ligands.

As a prosecution of our previous studies [42,43] a series of new ligands was designed and tested (Fig. 2). Starting from the good results obtained with β-lactam **A**, we synthesized fluorinated compounds **1** and **2**, as isosteric analogues of **A**, to probe the effect of the electronic properties by substituting fluorine atoms on the benzene ring adjacent to the urea. Compounds **3**–**5** would test the absence of the urea in comparison to the only amide group in a 4 or 5-membered heterocycle. Compound **5** would also test the absence of a carboxylic acid for the interaction with the metal ion-dependent adhesion site (MIDAS) of integrins. Compounds **6**–**10** have linear structures with respect to the cyclic amide in compound **A** thus probing the importance of steric constraint by cyclic structures. Moreover, molecules **6**–**8** with two carboxylic acid groups to resemble free tripeptides as analogues of the natural sequences as in Fig. 1, whereas compound **9** vs. **10** and **6** vs. **8** were synthesized to test the effect of a urea *vs* an amide group.

Therefore, in this study, we aimed to evaluate the binding affinity of the new synthesized ligands to $\alpha_4\beta_1$ integrin and their effects on $\alpha_4\beta_1$ integrin-mediated cell adhesion. Combining the experimental data with the chemical modifications introduced in the new compounds, we also performed a structure-activity relationship (SAR). Then, in cell adhesion assays, new ligands' selectivity was evaluated towards $\alpha_M\beta_2$, another leukocyte integrin, and $\alpha_5\beta_1$, an integrin heterodimer sharing the same β subunit of $\alpha_4\beta_1$. This analysis led to the identification of dual $\alpha_4\beta_1$-$\alpha_M\beta_2$ ligands that could have potential therapeutic applications in the field of anti-inflammatory drugs and anti-cancer immunotherapy. Lastly, the evaluation of the most potent $\alpha_4\beta_1$ integrin new ligands' effects on intracellular signalling allowed us to confirm agonist/antagonist behaviour as well as a differential regulation on diverse signalling cascades, supporting the idea of functional pathway selectivity for $\alpha_4\beta_1$ integrin.

2. Results and discussion

2.1. Chemistry

The synthesis of β-lactams **1**–**3** (Scheme 1) has a common racemic intermediate **11** obtained from the commercially available 4-acetoxy azetidinone by a substitution reaction with a Reformatsky reagent prepared *in situ* from benzyl bromoacetate in the presence of Zn in THF to give azetidinylacetate **11** in 65 % overall yields after flash chromatography (Scheme 1) [42]. To obtain the ureidic compounds **12** and **13**, compound **11** was acylated on the nitrogen atom with the corresponding isocyanates. These were prepared *in situ* from the corresponding amines by treatment with triphosgene in the presence of TEA, and immediately used (Scheme 1) [42]. The final racemic compounds **1** and **2** were obtained by hydrogenolysis of the benzyl esters in almost quantitative yields. For the synthesis of compound **14**, Boc-(4-aminophenyl)acetic acid was coupled to the intermediate **11** in the presence of HBTU and DIPEA. Hydrogenolysis of the benzylester (intermediate **15**) and deprotection of Boc-carbamate with trifluoroacetic acid (TFA) gave the final racemic compound **3** in good yields.

For the synthesis of chiral compounds **4** and **5** we started from commercially available enantiopure L-proline-benzyl ester **16** (Scheme 2). To obtain the intermediate **17**, the amine of proline was acylated with Boc-(4-aminophenyl)acetic acid in the presence of DCC and DMAP. Deprotection of the benzyl ester and of Boc-carbamate gave the desired chiral compound **4**. The intermediate **19** was obtained by acylation with *tert*-butyl(4-(isocyanatomethyl)phenyl)carbamate in the presence of TEA. After benzylester and *N*-Boc deprotection by hydrogenolysis, the ureidic intermediate underwent to an intramolecular cyclization to give the hydantoin **5**, as confirmed by mass spectrometry, mono- and 2D NMR analyses. Anyway, chiral compound **5** was tested against integrins and considered a negative control of the effect of a carboxylic acid residue present in all the other molecules reported here.

Compounds **6**, **7**, and **8** were obtained starting from commercially available enantiopure L-aspartic acid- or L-glutamic acid dibenzylesters **21** and **26**. A careful strategy for protecting the final carboxylic acid and the amine terminus was developed in order to choose those specific combinations to achieve full or partial deprotections as described in Scheme 3.

Finally, β-alanine benzyl ester **29** was coupled with Boc-(4-aminophenyl)acetic acid under typical conditions as EDC, HOBt, and TEA, to give compound **30**, which by hydrogenolysis and TFA treatment furnished the final compound **9**. Compound **32** was obtained from **29** and benzyl (4-(isocyanatomethyl)phenyl)carbamate, in turn prepared with the same conditions for isocyanates synthesis starting from 4-(Cbz-amino)benzylamine (Scheme 4). The selection of a *N*-Cbz group instead of *N*-Boc, allowed to obtain compound **10** in a single deprotection step, as an effective alternative with improved overall yields and step

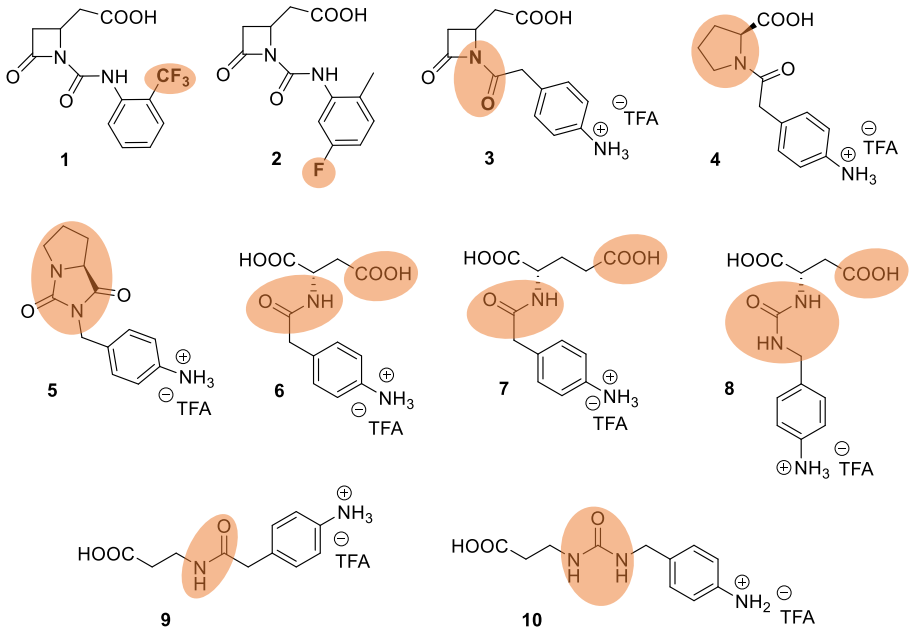

Fig. 2. Structures of new molecules designed to target leukocyte integrins, circular frames highlight the main modifications.

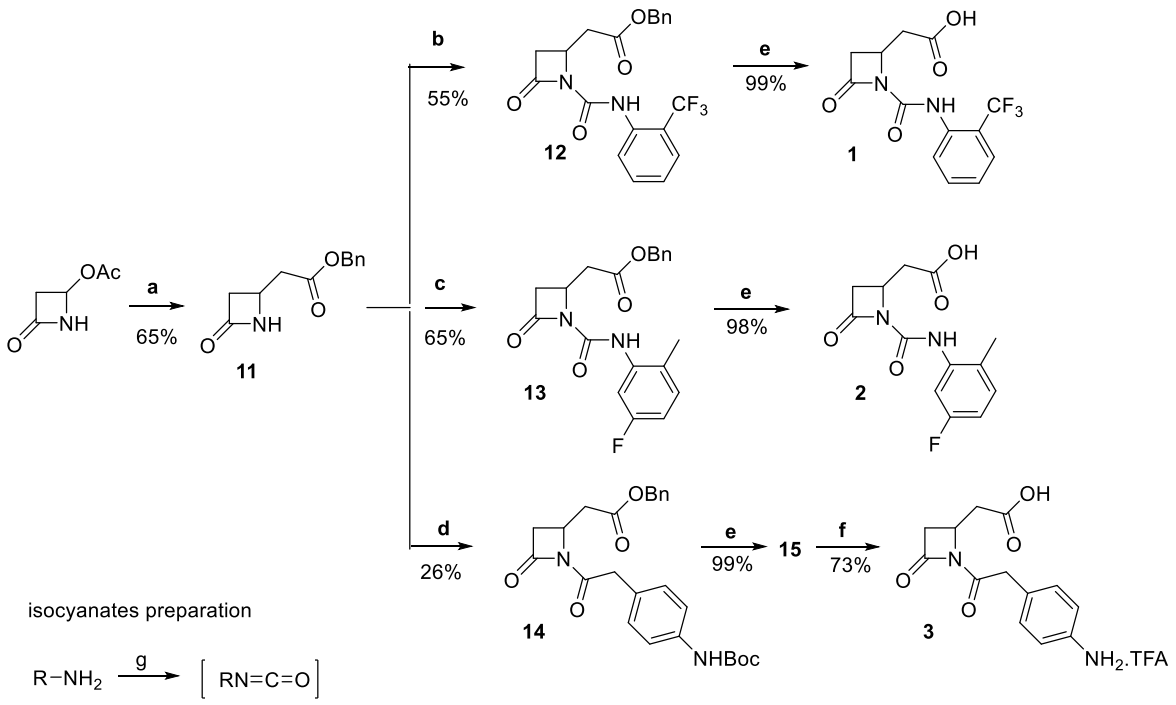

Scheme 1. Synthesis of compounds **1**, **2**, and **3**. Reagents and conditions: (a) Zn, TMSCl, benzyl bromoacetate, THF, 0 °C then rt, 3 h; (b) TEA, 1-isocyanato-2-(trifluoromethyl) benzene, DCM, 16 h, rt; (c) TEA, 4-fluoro-2-isocyanato-1-methylbenzene, DCM, 16 h, rt; (d) Boc-(4-aminophenyl)acetic acid, HBTU, DIPEA, DCM, 0 °C then rt, 24 h; (e) H_2, Pd/C (10 %), THF/MeOH 1:1, rt, 2 h; (f) TFA, DCM, 0 °C then rt, 1–4 h; (g) triphosgene, TEA, DCM, reflux, 4 h.

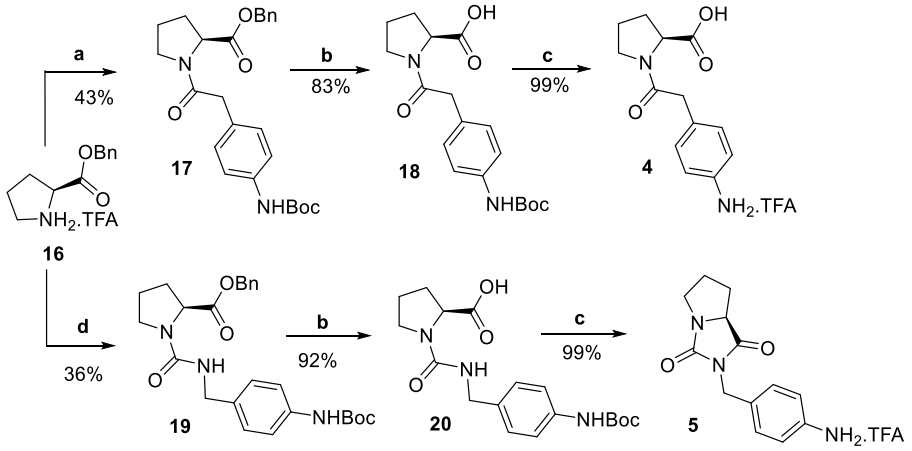

Scheme 2. Synthesis of target compounds **4** and **5**. Reagents and conditions: (a) Boc-(4-aminophenyl)acetic acid, TEA, DCC, DMAP, DCM, 0 °C then rt, 24 h; (b) H_2, Pd/C (10 % wt), THF/MeOH 1:1, rt, 2 h; (c) TFA, DCM, 0 °C then rt, 4 h; (d) TEA, *tert*-butyl(4-(isocyanatomethyl)phenyl)carbamate, DCM, 16 h, rt.

economy.

2.2. Pharmacological characterization of the new compounds

2.2.1. Evaluation of new ligands' affinity and potency towards $\alpha_4\beta_1$, $\alpha_5\beta_1$, and $\alpha_M\beta_2$ integrins

To measure the binding affinity towards $\alpha_4\beta_1$ integrin, the new compounds **1**–**10** were preliminarily tested in competitive binding experiments on intact Jurkat E6.1 cells. The ability of different concentrations of new β-lactam compounds to displace the fluorescently labelled ligand LDV-FITC from $\alpha_4\beta_1$ receptor was measured as K_i and results are collected in Table 1. Binding curves are provided in the Supporting Information (Fig. S1). The molecules **A** and **E** [42] were considered as reference compounds.

Analysing the results in Table 1, we observe that only 3 out of the newly synthesized 10 molecules behaved as ligands for $\alpha_4\beta_1$ receptor at a nanomolar level. By comparison with the parental compound **A**, fluorinated molecules **1** and **2** completely lost affinity against the receptor. The β-lactam compound **3** showed comparable affinity to that of compound **A**, thus demonstrating that the absence of the urea group did not interfere with the binding to $\alpha_4\beta_1$ integrin. The proline-based compound **4** showed the best affinity to the receptor at a sub-nanomolar level. It is interesting to note that **4** has the same number of C atoms as compound **3**, but in compound **4** the carboxylic acid that should interact at the metal ion-dependent adhesion site (MIDAS) of the integrin is directly anchored onto the 5-membered ring, thus with a lower conformational freedom than compound **3**. The only dicarboxylic acid recognized by the receptor is compound **8**, which showed an excellent affinity. This may be due to a longer distance between the acidic and the basic residues than those present in **6** or **7**, which allowed more favourable interactions at

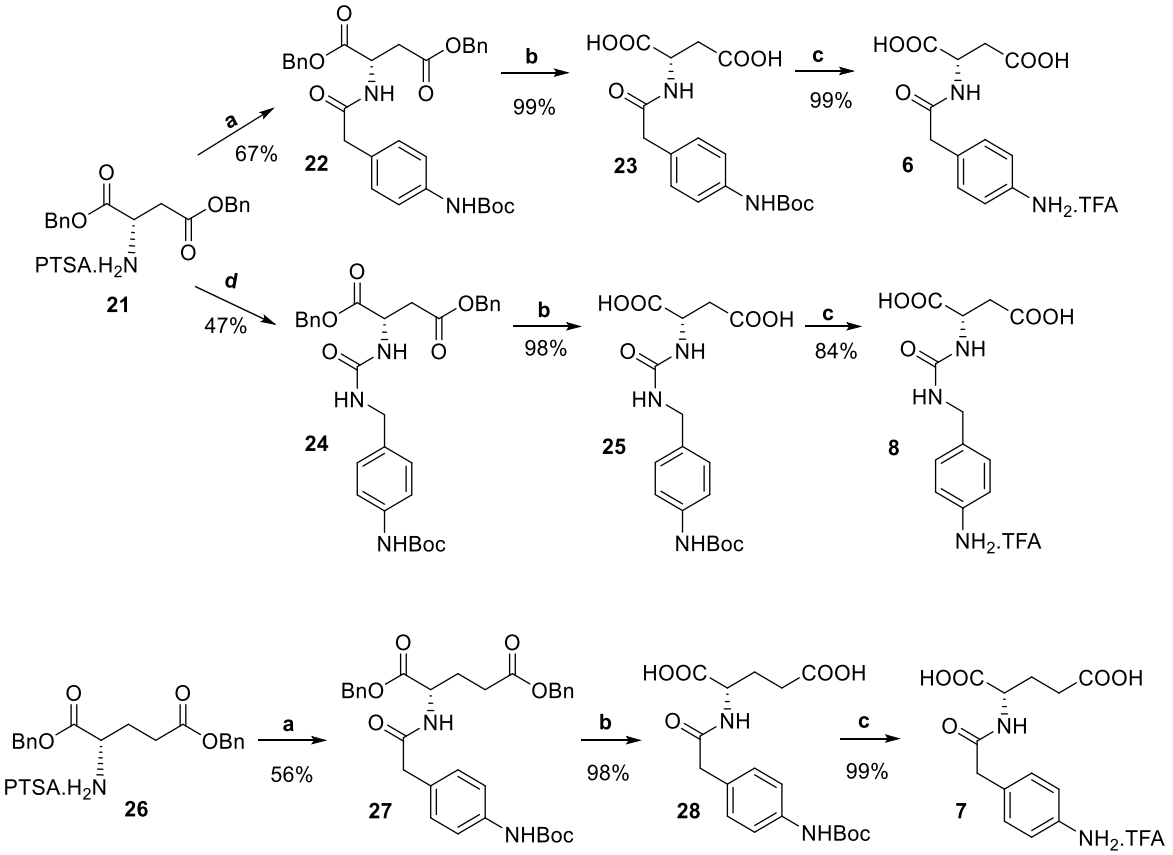

Scheme 3. Synthesis of compounds **6**–**8**. Reagents and conditions: (a) Boc-(4-aminophenyl)acetic acid, HOBt, EDC, TEA, DCM, 0 °C then rt, 24 h; (b) H_2, Pd/C (10 %), THF/MeOH 1:1, rt, 2 h; (c) TFA, DCM, 0 °C then rt, 1–4 h; (d) TEA then *tert*-butyl(4-(isocyanatomethyl)phenyl)carbamate, DCM, rt, 18 h.

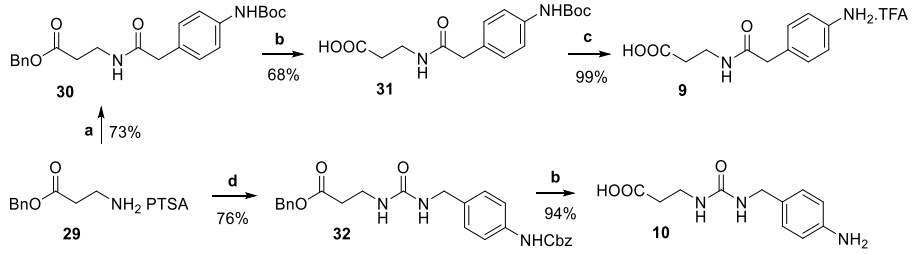

Scheme 4. Synthesis of target compounds **9**, and **10**. Reagents and conditions: (a) Boc-(4-aminophenyl)acetic acid, HOBt, EDC, TEA, DCM, 0 °C then rt, 24 h; (b) H_2, Pd/C (10 %), THF/MeOH 1:1, rt, 2 h; (c) TFA, DCM, 0 °C then rt, 1–4 h; (d) TEA, benzyl (4-(isocyanatomethyl)phenyl) carbamate, DCM, rt, 18 h.

Table 1
Affinity of compounds **1**–**10** for $\alpha_4\beta_1$ integrin obtained via competitive binding experiments on intact Jurkat E6.1 cells *vs* LDV-FITC. Values are reported as K_i (nM).[a]

Compound number	Binding affinity K_i (nM)	Compound number	Binding affinity K_i (nM)
1	>5000	**7**	>5000
2	>5000	**8**	7.7 ± 1.3
3	9.8 ± 2.5	**9**	>5000
4	0.13 ± 0.09	**10**	>5000
5	>5000	**A**	9.8 ± 0.8[b]
6	>5000	**E**	498 ± 27[b]

[a] Values represent the mean ± SD of three independent experiments, in duplicate.
[b] Data previously reported in ref. 42.

the receptor, and the presence of the urea group with respect to **6**. Compounds **9** and **10** derived from β-alanine were not able to bind to $\alpha_4\beta_1$.

To further characterize the new molecules' effects on $\alpha_4\beta_1$-mediated cell adhesion, Jurkat E6.1 cells, endogenously expressing $\alpha_4\beta_1$, were allowed to adhere in 96-well plates coated with FN or VCAM-1, in the presence of increasing concentrations (10^{-10} to 10^{-4} M) of the new compounds **1**–**10**, as described in the Experimental Section. Furthermore, compounds' selectivity was assessed towards the leukocyte integrin $\alpha_M\beta_2$, expressed on HL-60 cells, and $\alpha_5\beta_1$, present on K562 cell surface, and sharing the β_1 subunit with the heterodimer $\alpha_4\beta_1$. The results obtained from cell adhesion assays are collected in Table 2 and concentration-response curves are provided in the Supporting Information (Fig. S2−S5). Data of reference compounds **A** and **E** [42] were reported for comparison. In addition, Fig. 3 shows the heatmap of the adhesion index, i.e. a measure of the agonistic or antagonistic behaviour of the new compounds [49]. Agonists are defined by adhesion index >1

(displayed in shades of purple), antagonists by adhesion index <1 (displayed in shades of blue), and integrin ligands not significantly modulating cell adhesion by adhesion index approximately = 1.

The substitution of some hydrogen atoms of the parental compound **A** with fluorine atoms in compounds **1** and **2** completely changed the selectivity for the integrin heterodimer. Fluorinated derivatives **1** and **2** confirmed their inactivity in cell adhesion tests against $\alpha_4\beta_1$, however, they were both active ligands against $\alpha_5\beta_1$. In particular, compounds **1** and **2** showed opposite activities for $\alpha_5\beta_1$, being an antagonist and an agonist, respectively, both with very good potency. Additionally, compound **2** behaved as a selective agonist for the $\alpha_5\beta_1$ integrin. On the contrary, **1** showed an interesting agonistic activity also towards $\alpha_M\beta_2$.

Table 2
Effects of Compounds **1**–**10** on Integrin-Mediated Cell Adhesion performed on Jurkat E6.1 cells for $\alpha_4\beta_1$, K562 cells for $\alpha_5\beta_1$, and HL-60 cells for $\alpha_M\beta_2$.[a,b]

Compound number	Structure	Jurkat/FN $\alpha_4\beta_1$	Jurkat/VCAM-1 $\alpha_4\beta_1$	K562/FN $\alpha_5\beta_1$	HL60/Fg $\alpha_M\beta_2$
1	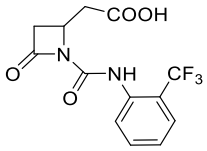	>5000	>5000	44.1 ± 7.5 **antagonist**	19.0 ± 5.1 **agonist**
2	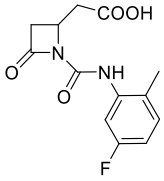	>5000	>5000	45.98 ± 7.92 **agonist**	>5000
3	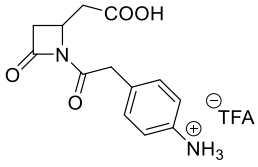	268 ± 41 **antagonist**	594 ± 16 **antagonist**	>5000	34 ± 7 **antagonist**
4	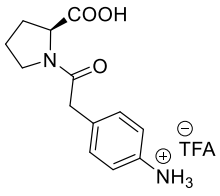	310 ± 41 **antagonist**	15 ± 3 **antagonist**	>5000	23 ± 5 **agonist**
5	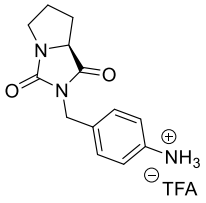	19 ± 2 **agonist**	25 ± 3 **agonist**	4.8 ± 3.4 **agonist**	>5000
6	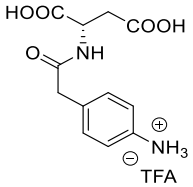	>5000	>5000	>5000	>5000
7	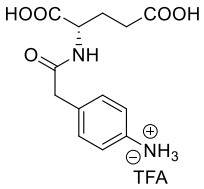	>5000	>5000	361 ± 53 **agonist**	>5000

(*continued on next page*)

Table 2 (*continued*)

Compound number	Structure	Jurkat/FN $\alpha_4\beta_1$	Jurkat/VCAM-1 $\alpha_4\beta_1$	K562/FN $\alpha_5\beta_1$	HL60/Fg $\alpha_M\beta_2$
8	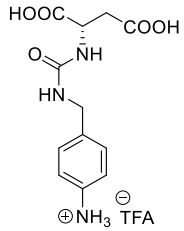	144 ± 30 **antagonist**	325 ± 21 **antagonist**	>5000	1.4 ± 0.2 **agonist**
9	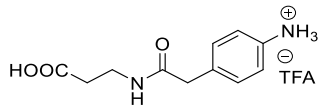	>5000	>5000	>5000	>5000
10	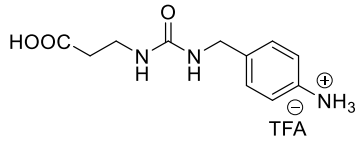	>5000	>5000	>5000	>5000
A	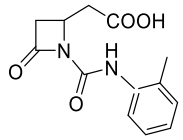	15.6 ± 1.1 **agonist**	12.9 ± 0.6[d] **agonist**	>5000[d]	nd[c]
E	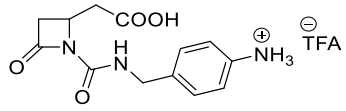	404 ± 3 **antagonist**	574 ± 2[d] **antagonist**	44.5 ± 2.6 [d] **agonist**	>5000

[a] Data are presented as EC_{50} for agonists and IC_{50} for antagonists (nM).
[b] Values represent the mean ± SD of three independent experiments performed in quadruplicate.
[c] nd: not detected.
[d] Data previously reported in ref. 42.

Fluorine substitution is commonly used in medicinal chemistry to improve bioavailability, metabolic stability, and interactions with biological targets [50,51]. The substitutions of CH_3 to CF_3 or CH to CF in combination with the high electronegativity of the F atom could induce changes in bond polarization, molecular conformation, and enhancement of lipophilicity. Moreover, the presence of a fluorine atom proximal to an amide could modify the basicity of that group thus changing its H-bond properties to some extent [50,51]. These actions of F atoms in **1** and **2** were determinant to null the activity against $\alpha_4\beta_1$. On the contrary, the effects of the F atoms were able to activate the two compounds against $\alpha_5\beta_1$. Concerning the selectivity of **2** against $\alpha_5\beta_1$ compared to its inactivity toward $\alpha_4\beta_1$, the major role in this regulation and recognition could be tentatively ascribed to the presence of a lipophilic pocket in the α_5 subunit [52–54]. In the fluorinated ligands **1** and **2**, enhanced lipophilicity by the presence of F atoms linked with an aryl group and next to the COOH residue could account for the $\alpha_5\beta_1$ selectivity. The switch from antagonism of **1** to agonism of **2** against $\alpha_5\beta_1$ was quite difficult to explain at the molecular level. Most integrins are present in a bent-closed conformation with low affinity for ligands on resting cells, but they move to a high-affinity extended-open state on binding to their natural ligands [55]. Springer and co-workers demonstrated for $\alpha_{IIb}\beta_3$ integrin that closing inhibitors favouring the bent-closed conformation contain a polar nitrogen atom that stabilizes a water molecule via hydrogen bonds that intervenes between a serine residue and the metal in the metal-ion-dependent adhesion site (MIDAS) [56]. The expulsion of this water molecule should be a condition for the transition to the extended open conformation. Following this model, an agonist should be that ligand able to displace the water molecule from the coordination of MIDAS. This model was validated even for $\alpha_4\beta_1$ and could be tentatively extended to other integrins [56]. In our case, the presence of a CF_3 group in compound **1** next to the urea could increase the polarization of the NH group, thus favouring the stabilization of a water molecule in the MIDAS. Following the model proposed by Springer, this effect could account for the stabilization of a closed conformation of the integrin and thus for the antagonism of this molecule. It is noteworthy that the development of selective $\alpha_5\beta_1$ integrin antagonist ligands may have great therapeutic potential in the treatment of ischemic stroke injuries [57]. On the contrary, in compound **2** the fluorine in meta position of the aryl group did not influence the polarization of the NH and this could favour the expulsion of the water molecule from MIDAS, so that this compound worked as an agonist.

The $\alpha_M\beta_2$ integrin plays an important role in a diversity of immunological processes notwithstanding it is particularly promiscuous in ligand selectivity and functional profile [58]. It was recognized that the α_MI-domain is responsible for a broad ligand recognition with a preference for short peptides enriched with a basic residue flanked by a hydrophobic group [58–60]. The presence of the ortho lipophilic CF_3 group next to the urea in compound **1** could account for the activity as an agonist of $\alpha_M\beta_2$ as a result of the preference observed for peptides. Activation of the integrin $\alpha_M\beta_2$ showed anti-inflammatory activity in animal models of some human diseases, and this action was recognized as a novel therapeutic strategy [61].

The lack of the urea group in compound **3** did not have any effect against $\alpha_4\beta_1$ because **3** showed the same activity as **E.** However, **3** was

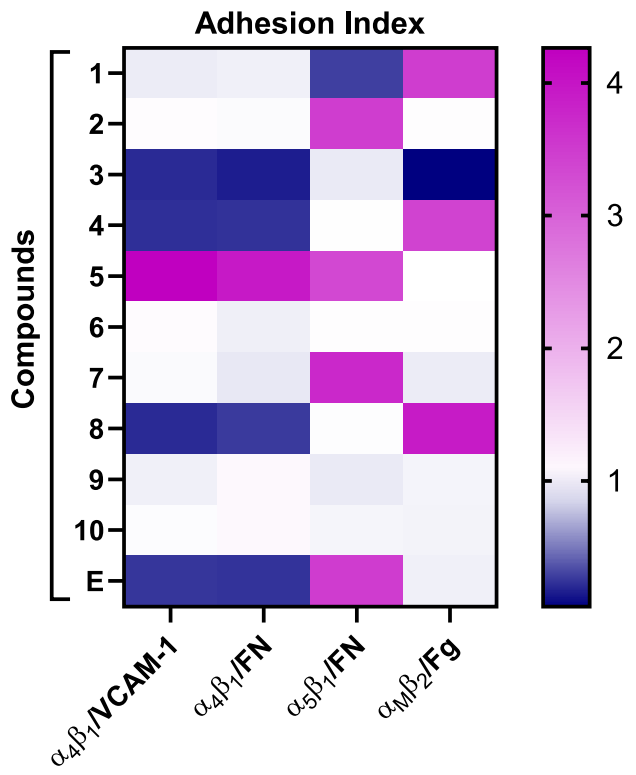

Fig. 3. Heatmap of adhesion index: antagonists are displayed in shades of blue and agonist compounds are shown in shades of purple. The adhesion index is calculated as the ratio between the number of adhered cells in the presence of the highest new compound concentration (10^{-4} M) and the number of adhered vehicle-treated cells. (For interpretation of the references to colour in this figure legend, the reader is referred to the Web version of this article.)

inactive against $\alpha_5\beta_1$ whereas **E** was a good ligand instead. This result evidenced the importance of the urea NH for recognition by $\alpha_5\beta_1$ integrin. The cationic aniline together with the carboxylic acid enabled compound **3** to act as an antagonist of $\alpha_M\beta_2$.

Cell adhesion tests confirmed compound **4** as a good ligand of $\alpha_4\beta_1$ integrin with the behaviour of antagonist; on the contrary, it was able to increase cell adhesion mediated by $\alpha_M\beta_2$ at nanomolar range.

The activity of compound **5** in cell adhesion assays against $\alpha_4\beta_1$ and $\alpha_5\beta_1$was quite unexpected. This compound in fact was not able to bind to $\alpha_4\beta_1$ as shown in LDV-FITC competitive binding assays (Table 1), but it significantly increased $\alpha_4\beta_1$-mediated cell adhesion. In addition, **5** was an agonist also for $\alpha_5\beta_1$. Because of the absence of a COOH residue and thus the lack of a possible binding interaction at the MIDAS, the behaviour of **5** could be tentatively explained by the interaction with an allosteric site able to activate both integrins and to foster the cell adhesion process. Moreover, it has been shown that the binding of an allosteric ligand could alter the relative stabilities of integrin conformations [62], and for an allosteric agonist such as **5**, it could favour an active extended-open conformation of the integrin that promote cell adhesion.

Concerning the two aspartic-derivatives **6** and **8** only the latter conserved a certain activity against $\alpha_4\beta_1$; interestingly **8** showed an excellent potency in activating $\alpha_M\beta_2$ integrin at a nanomolar range. On comparing the glutamate derivative **7** with the aspartate one **6**, only **7** with a longer chain showed some activity against $\alpha_5\beta_1$.

Unexpectedly, the two β-alanine derivatives **9** and **10** were completely inactive in modulating cell adhesion, whereas in other molecules recently developed, the insertion of a β-amino acid as β-alanine in a short peptide was successful [59].

Summarizing, the structure-activity relationships (SAR) observed in the series of new compounds:

- respect the model compound **E**, the insertion of F atoms switched the integrin selectivity from $\alpha_4\beta_1$ to $\alpha_5\beta_1$, and $\alpha_M\beta_2$, with compound **2** being a potent and selective agonist ligand of $\alpha_5\beta_1$;
- the absence of the urea group on the β-lactam nitrogen atom switched the selectivity to integrin $\alpha_5\beta_1$ from that of the model compound **E** to $\alpha_4\beta_1$;
- the expansion of the ring from 4 to 5 members as from β-lactam to proline did not have influence on the integrin selectivity, but on reducing the flexibility of the carboxylic acid residue, proline compound **4** resulted an agonist ligand of $\alpha_M\beta_2$ with respect to the β-lactam compound **3** which was an antagonist;
- alicyclic compounds are far less active than the cyclic counterparts with the exception of compound **8** which was the best agonist ligand of $\alpha_M\beta_2$ in the series of new compounds.

The modulation of $\alpha_M\beta_2$-mediated cell adhesion by compounds **1**, **3**, **4**, and **8** is particularly interesting because it was demonstrated that activation of $\alpha_M\beta_2$ reduces inflammation [61] and could reprogram immunosuppressive responses in myeloid cells and thus overcome resistance to immunotherapy in cancer diseases [44,63]. Accordingly, previous studies showed that $\alpha_M\beta_2$ agonists induced the repolarization of tumor-associated macrophages, the reduction of tumor-infiltrating immunosuppressive myeloid cells, thus improving anti-tumor T cell immunity in a model of pancreatic ductal adenocarcinoma [44,45]. These effects can be therapeutically advantageous to overcome resistance to checkpoint inhibitor cancer immunotherapy. Therefore, further studies will be performed to better characterize the effects of these compounds on $\alpha_M\beta_2$ integrin functions, also in human primary immune cells and tumor-infiltrating immune cells.

Although the primary aim of the present study was to identify selective $\alpha_4\beta_1$ integrin compounds, some newly synthesized molecules proved to be dual $\alpha_4\beta_1$-$\alpha_M\beta_2$ ligands; in particular, **3** was a dual antagonist, while **4** and **8** were $\alpha_4\beta_1$ antagonists/$\alpha_M\beta_2$ agonists. Targeting simultaneously both $\alpha_4\beta_1$ and $\alpha_M\beta_2$ integrins could be therapeutically useful for the treatment of chronic inflammatory diseases [29,64] and some types of cancer [44,65,66]. What should be better understood is the activity (agonist or antagonist) at the integrin receptor that is needed to mediate the therapeutic effects.

However, the agonism or antagonism of integrin ligands is still a complex and unresolved issue because it was experimentally observed that several factors influence the behaviour of small molecules in activating or deactivating integrins [67]. In some cases, it was observed a dose-dependent switch from agonism at low concentrations to antagonism at higher concentrations [68] Moreover, it was observed that even the reorganization of the transmembrane domain of integrins could be key to the understanding of the agonistic properties of integrin ligands at substoichiometric concentrations [69]. In other cases, the ligand changed its behaviour depending on specific cations in solution: Ca^{2+} and Mg^{2+} stimulate the activation against $\alpha_L\beta_2$. whereas Mn^{2+} deactivates [70]. It was also observed that for $\alpha_{IIb}\beta_3$-ligand binding only the interaction with the β subunit was enough to allow activation of the integrin [71].

Notwithstanding those different factors, depending on the pathological context, both agonists and antagonists, activating or blocking integrin functions respectively, could be therapeutically useful.

2.2.2. Effects of the most promising new compounds on $\alpha_4\beta_1$ integrin-mediated intracellular signalling pathways

Integrins transmit signals bidirectionally across the cell membrane and induce the activation of intracellular downstream events, including MAPK and Akt pathways, thus mediating essential cell functions, such as migration, cell proliferation, cell adhesion and differentiation [72]. To better characterize the most promising $\alpha_4\beta_1$ integrin ligands and confirm

their agonist or antagonist behaviour, we evaluated the effects of compounds **3**, **4**, **5**, and **8** on $\alpha_4\beta_1$ integrin-mediated activation of MAPK and Akt pathways. To this aim, Jurkat E6.1 cells were pre-exposed to different concentrations (10^{-7} - 10^{-9} M) of the most active $\alpha_4\beta_1$ integrin antagonists identified in cell adhesion assays (**3**, **4**, and **8**), and then treated with the endogenous ligand FN (10 μg/mL). On the contrary, for the agonist **5**, the activation of integrin-mediated intracellular signalling was analysed in the absence of FN, in order to confirm compound's ability to mimic the effects of the endogenous ligands activating EKR1/2, Akt, and JNK kinases.

As shown in Fig. 4, $\alpha_4\beta_1$ integrin antagonists **3**, **4**, and **8** were able to significantly prevent FN-induced activation of ERK1/2 at all concentrations tested, confirming their antagonistic behaviour. As regards Akt signalling, only compounds **3** and **4** reduced kinase phosphorylation activated by FN; in addition, both antagonists counteracted the FN-activating effect on JNK, although only at the highest concentrations. Thus, showing to be less effective in preventing the activation of JNK intracellular signalling pathway. In contrast, compound **8** did not prevent Akt and JNK activation.

Interestingly, the $\alpha_4\beta_1$ agonist **5** significantly activated integrin-mediated intracellular pathways in Jurkat E6.1 cells, leading to an increase in ERK1/2 and Akt phosphorylation (Fig. 5), and confirming its activity as an allosteric agonist; on the contrary, we did not observe any effects of **5** on JNK activation.

Given the differential effects of compounds **3**, **4**, **5**, and **8** on various intracellular signaling pathways, we calculated the pathway selectivity index (PSI) to eventually define them as biased ligands. PSI describes the degree of functional selectivity towards a specific intracellular signaling pathway. As shown in Fig. 6, antagonists **3**, **4**, and **8** displayed a strong preference in blocking ERK1/2 signaling pathways over both Akt and JNK (very low PSI values). Moreover, all three compounds mentioned above showed no functional selectivity as regards to Akt/JNK signaling cascades. On the contrary, $\alpha_4\beta_1$ agonist **5** had a strong preference in activating ERK1/2 kinase over JNK (PSI values very high), but only a moderate preference towards Akt over JNK and no functional selectivity comparing ERK/Akt activation.

Overall, the results obtained in this study on the $\alpha_4\beta_1$ antagonists **3**, **4**, and **8**, and the agonist **5** confirm their ability to bind to the receptor and modulate its functions, such as cell adhesion and intracellular signalling. In addition, their ability to differentially modulate signal transduction supports the idea that biased ligands, able to target specifically a definite integrin conformation and downstream signalling cascades, can be defined also for integrins [73,74]. Biased ligands could offer the potential for treatments with enhanced efficacy and minimal side effects. Moreover, compound **5** may be considered as an allosteric agonist of $\alpha_4\beta_1$, as it is able to activate the downstream signalling regardless of its inability to bind to the same site of LDV, thus suggesting the presence of an allosteric site, already described for other integrins [62,75–77]. Nevertheless, further studies are needed to better unravel the underlying molecular determinants of new integrin ligands developed in this study.

3. Conclusions

In conclusion, we designed and synthesized a series of novel compounds to target firstly $\alpha_4\beta_1$ integrin. The design of new molecules was inspired by β-lactam **A**, taken as a model of a selective and potent agonist of integrin $\alpha_4\beta_1$. Three compounds **3**, **4**, and **8,** out of ten, showed excellent binding affinities (Ki < 10 nM) in competitive binding experiments on intact Jurkat E6.1 cells, being able to displace the fluorescent ligand LDV-FITC from $\alpha_4\beta_1$ receptor. All new compounds were then submitted to cell adhesion tests on Jurkat E6.1 for $\alpha_4\beta_1$, K562 cells for $\alpha_5\beta_1$, and HL-60 for $\alpha_M\beta_2$ integrin. Fluorinated compounds **1** and **2** showed selective activities against $\alpha_5\beta_1$ and/or $\alpha_M\beta_2$. Compounds **3**, **4**, and **8** confirmed their activities against $\alpha_4\beta_1$ and even for $\alpha_M\beta_2$, but not for $\alpha_5\beta_1$, thus being considered as dual $\alpha_4\beta_1$-$\alpha_M\beta_2$ ligands with potential therapeutically relevant applications. Compound **5** showed a peculiar behaviour which could be ascribed to interaction with allosteric binding sites of $\alpha_4\beta_1$ and $\alpha_5\beta_1$. Moreover, antagonists **3**, **4**, **8**, and agonist **5** were able to differentially modulate $\alpha_4\beta_1$ integrin-mediated intracellular signalling, with a functional selectivity preference over ERK1/2 intracellular signaling. Thus, reinforcing the idea of biased ligands for $\alpha_4\beta_1$ that could have enhanced therapeutic efficacy with reduced side effects. Nevertheless, further studies are needed to better unravel the therapeutic effects of functional selectivity in the frame of integrin ligands.

The most active ligands identified in this study can be considered as potential lead compounds for the development of new drugs useful in the treatment of inflammatory diseases and some types of cancer expressing $\alpha_4\beta_1$ integrin.

4. Experimental Section

4.1. Chemistry

Commercial reagents were used as received without additional purification. ^{1}H and ^{13}C NMR spectra were recorded with an INOVA 400 and a Bruker Avance 600 MHz instrument with a 5 mm probe. All chemical shifts were quoted relative to deuterated solvent signals (δ in ppm and J in Hz). Polarimetric analyses were conducted on Unipol L 1000 "Schmidt−Haensch" polarimeter at 598 nm. ATR-FTIR spectra of pure compounds were recorded with a Bruker Alpha instrument or with an Agilent Technologies CARY 630 FTIR, in transmittance mode with a 4 cm^{-1} resolution in the 4000-400 cm^{-1} range. The purities of the target compounds **1**–**10** were assessed by analytical HPLC analyses Agilent Technologies HP1100 instrument. HRMS: Waters Xevo G2-XS QTof (ESI-APCI). HPLC-MS: Agilent Technologies HP1100 instrument, coupled with an Agilent Technologies MSD1100 single-quadrupole mass spectrometer, full scan mode from $m/z = 50$ to 2600, in positive or negative ion mode and equipped with a ZORBAX-Eclipse XDB-C8 Agilent Technologies column; mobile phase, H_2O/CH_3CN, 0.4 mL/min; gradient from 30 to 80 % of CH_3CN in 8 min, 80 % of CH_3CN until 25 min.

Compounds **E** and **11** were synthesized according to reported procedures [42]. 2-(4-((*tert*-butoxycarbonyl)amino)phenyl)acetic acid was obtained from phenylacetic acid and di-*tert*-butyldicarbonate in aqueous NaOH, according to ref [78]. Compound **16** was synthetized in two steps from N-Boc proline [79,80]. Isocyanates were prepared from the corresponding amines in the presence of triphosgene and TEA in DCM at reflux [81]. Starting amines 2-(trifluoromethyl)benzenamine and 3-fluoro-6-methylaniline are commercially available while *tert*-butyl (4-(aminomethyl)phenyl)carbamate and 4-(aminomethyl)-N-(benzyloxycarbonyl)phenylamine were synthetized according to ref. [82,83], respectively.

4.1.1. General procedure for the synthesis of benzylesters (GP1)

A dicarboxylic acid compound (1 equiv) was dissolved in toluene (2,9 mL/mmol, 1:1 v/v), under a nitrogen atmosphere and benzyl alcohol (6.5 equiv) and *para*-toluensulfonic acid (1.4 equiv) were added. The solution was then stirred at reflux for 24 h. After the complete consumption of the starting material (TLC monitoring), the reaction mixture was cooled to room temperature and evaporated; then MeOH (2 mL) was added and warmed to dissolve the residue. Then Et_2O (8 mL) was added, and finally the resulting suspension was filtered.

4.1.2. General procedure for hydrogenolysis (GP2)

A benzyl ester (1 equiv) was dissolved in a mixture of THF and MeOH (22 mL/mmol, 1:1 v/v), and Pd/C (10 % w/w) was added. The solution was then stirred under a H_2 atmosphere (1 atm) at room temperature. After a complete consumption of the starting material (TLC monitoring, 2 h) the reaction mixture was filtered through Celite and concentrated in vacuum. The crude was then triturated with a few drops of pentane to afford the desired carboxylic acid.

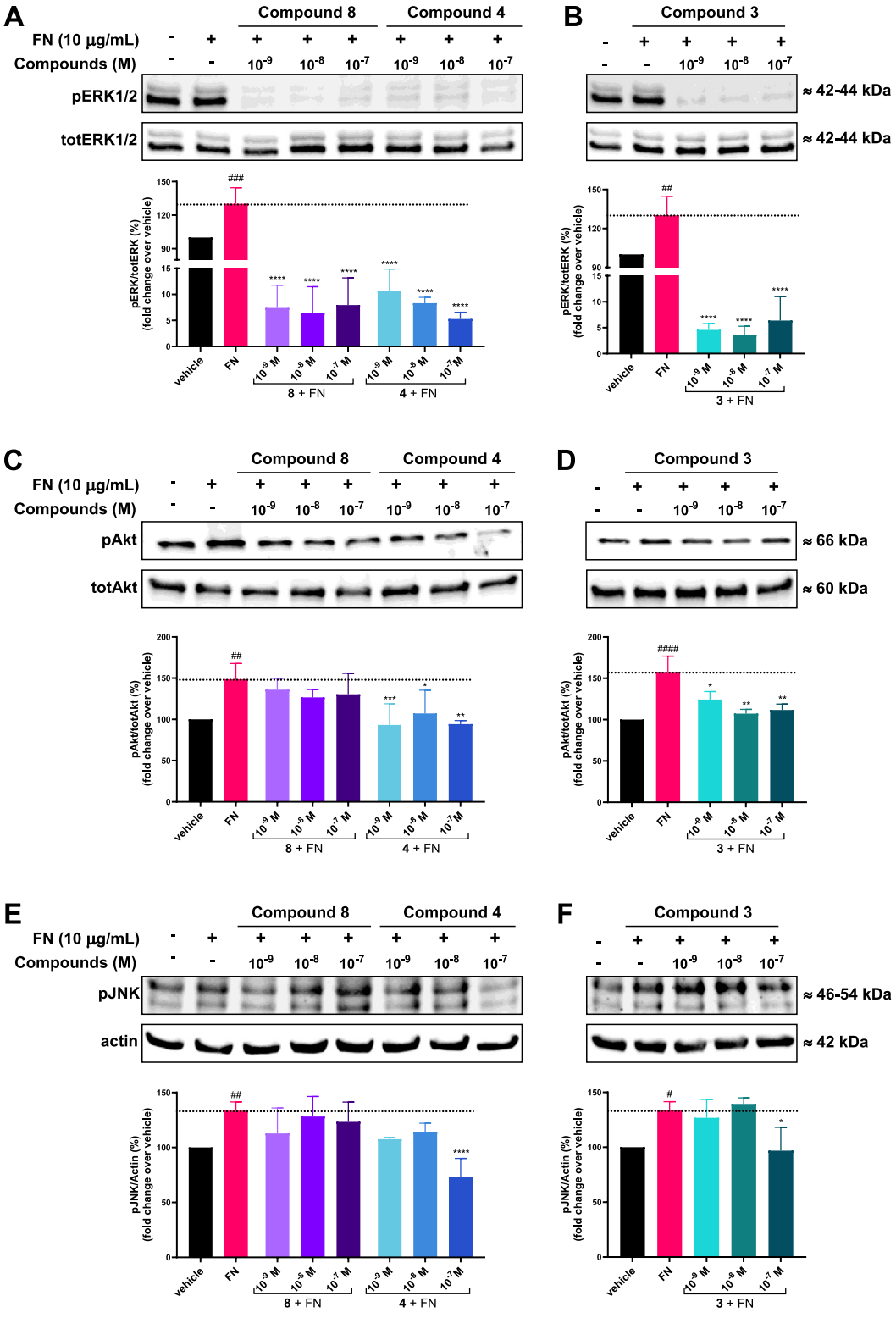

Fig. 4. Effects of the most potent new $\alpha_4\beta_1$ integrin antagonists on integrin-mediated intracellular signalling. Integrin antagonists **3**, **4**, and **8** were able to significantly prevent FN-induced $\alpha_4\beta_1$ integrin-dependent activation of ERK1/2 (A, B). Conversely only compounds **3** and **4** reduced FN-induced Akt (C, D) and JNK phosphorylation (E, F). As shown in the representative Western blot images, FN induced significant activation of ERK1/2, Akt, and JNK, if compared to vehicle-treated cells (vehicle). The graphs represent densitometric analysis of the bands (mean ± SD; three independent experiments). The amount of phosphorylated kinases (pERK1/2 or pAkt) was normalized to that of the corresponding total kinase (totERK1/2 or totAkt); phospho-JNK (pJNK) was normalized to actin. *$*p < 0.05$, **$p < 0.01$, ***$p < 0.001$, ****$p < 0.0001$ vs. vehicle; #$p < 0.05$, ##$p < 0.01$, ###$p < 0.001$, ####$p < 0.0001$ vs. FN* (Dunnett's test after ANOVA).

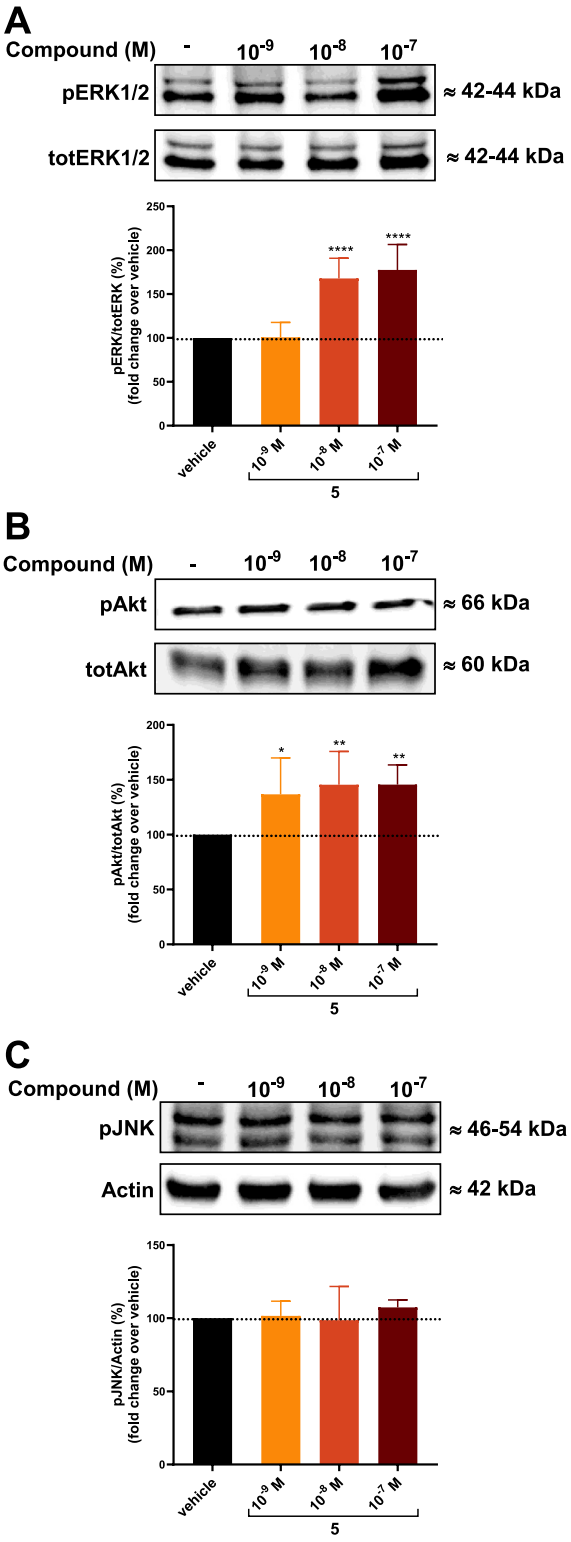

Fig. 5. Effects of the $\alpha_4\beta_1$ integrin agonist **5** on integrin-mediated intracellular signalling. Compound **5** significantly induced $\alpha_4\beta_1$ integrin-mediated activation of ERK1/2 (A) and Akt (B). Conversely, **5** showed no effects on JNK phosphorylation. The graphs represent the densitometric analysis of the bands (mean ± SD; three independent experiments). The amount of phosphorylated kinases (pERK1/2 or pAkt) was normalized to that of the corresponding total kinase (totERK1/2 or totAkt); phospho-JNK (pJNK) was normalized to actin. *$p < 0.05$, **$p < 0.01$, ****$p < 0.0001$ *vs. vehicle* (Dunnett's test after ANOVA).

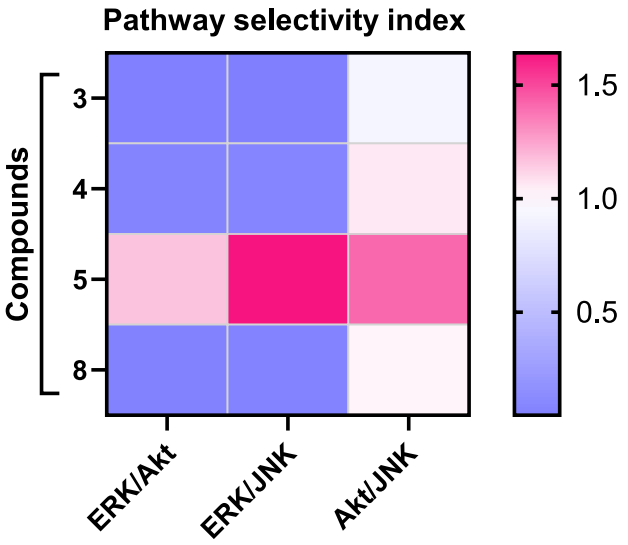

Fig. 6. Heatmap of pathway selectivity index (PSI): preference for blocking a specific pathway is displayed in shades of lilac, and preference in activating a specific kinase is shown in shades of magenta. The PSI is calculated as the ratio between AUC values of two kinases as described in the Experimental section. (For interpretation of the references to colour in this figure legend, the reader is referred to the Web version of this article.)

4.1.3. General procedure for N-Boc-deprotection (GP3)

A N-Boc-protected compound (1 equiv) was dissolved in DCM (18.5 mL/mmol) under nitrogen atmosphere, and trifluoroacetic acid (TFA) (4 equiv) was added dropwise at 0 °C. New TFA aliquots were added each 60 min at 0 °C until a complete conversion (HPLC or TLC monitoring). The solvent was removed under reduced pressure, and the crude was triturated with few drops of pentane to afford the resulting deprotected compound.

4.1.4. General procedure for coupling reaction with EDC-HOBt (GP4)

To a solution of amine (1.2 equiv) dissolved in DCM (6.5 mL/mmol) under a nitrogen atmosphere, anhydrous TEA (1.2 equiv) was added dropwise. The reaction was left for 20 min. At the same time, in a second round-bottom flask, the carboxylic acid (1 equiv) was dissolved in DCM (4.5 mL/mmol), and the solution of the first round-bottom flask was dropped. Then HOBt (0.5 equiv) and EDC (1 equiv) were added at 0 °C. The solution was warmed to rt and left under stirring. After complete consumption of the starting material (18 h, TLC monitoring), the mixture was quenched with H_2O and extracted with DCM The organic layer was dried over Na_2SO_4, concentrated in vacuum, and purified by flash chromatography.

4.1.5. 2-(4-Oxo-1-((2-(trifluoromethyl)phenyl)carbamoyl)azetidin-2-yl) acetic acid (1)

Following GP2, compound **12** (43 mg, 0.106 mmol, 1 equiv), in the presence of Pd/C (4.3 mg, 10 % wt) in 2.4 mL of THF:MeOH, gave compound **1** (33 mg, 0.104 mmol) in 99 % yield as a white solid, after trituration with pentane and diethylether. Purity by HPLC ($\lambda = 254$ nm): 94,5 %. ^{1}H NMR (400 MHz, CD_3OD) δ 8.09 (d, $J = 8.2$ Hz, 1H), 7.68 (dd, $J = 7.9$, 1.5 Hz, 1H), 7.67–7.55 (m, 1H), 7.31 (t, $J = 7.7$ Hz, 1H), 4.43 (ddt, $J = 9.1$, 6.3, 3.4 Hz, 1H), 3.39 (dd, $J = 16.2$, 5.8 Hz, 1H), 3.18 (dd, $J = 16.6$, 3.8 Hz, 1H), 3.04 (dd, $J = 16.2$, 3.0 Hz, 1H), 2.81 (dd, $J = 16.5$, 8.8 Hz, 1H). ^{19}F NMR (CD_3CD, 377 MHz) δ −62.65 (s). ^{13}C NMR (100 MHz, CD_3OD) δ 173.9 (bs), 168.9, 149.7, 135.8 (q, $J = 1.9$ Hz), 134.1 (q, $J = 1.2$ Hz), 127.2 (q, $J = 5.4$ Hz), 125.9, 125.8 (q, $J = 274.0$ Hz), 125.7, 122.0 (q, $J = 30.0$ Hz), 49.4, 43.6, 37.5 (bs). HPLC-MS (ESI^+): $t_R = 1.76$ min; m/z = 339.0 $[M+Na]^+$, 655.0 $[2\ M + Na]^+$. HRMS (ESI) m/z:

$[M+Na]^+$ calcd for $C_{13}H_{11}F_3N_2NaO_4$339.0569; found 339.0562. ATR-FTIR (cm^{-1}): 3338, 2961, 1775, 1717, 1618, 1553, 1458, 1322, 1287, 1245, 1173, 1117, 1059, 1036, 766, 652, 463.

4.1.6. (1-((5-fluoro-2-methylphenyl)carbamoyl)-4-oxoazetidin-2-yl)acetic acid (2)

Following GP2, compound **13** (23 mg, 0.062 mmol, 1 equiv), in the presence of Pd/C (2.3 mg, 10 % wt) in 1.4 mL of THF:MeOH, gave compound **2** (17 mg, 0.0061 mmol) in 98 % yield as a white solid after trituration with pentane and diethylether. Purity by HPLC (λ = 254 nm): 96 %. ^{1}H NMR (400 MHz, CD_3OD) δ 7.76 (dd, J = 11.2, 2.7 Hz, 1H), 7.18 (dd, J = 8.5, 6.4 Hz, 1H), 6.75 (td, J = 8.4, 2.7 Hz, 1H), 4.42 (tt, J = 5.6, 3.1 Hz, 1H), 3.38 (dd, J = 16.4, 6.9 Hz, 1H), 3.19 (dd, J = 16.5, 3.8 Hz, 1H), 3.02 (dd, J = 16.1, 3.0 Hz, 1H), 2.80 (dd, J = 16.5, 8.8 Hz, 1H), 2.24 (s, 4H). ^{13}C NMR (100 MHz, CD_3OD) δ 173.9 (bs), 169.2, 162.7 (d, J = 240.7 Hz), 149.6, 138.1 (d, J = 11.4 Hz), 132.3 (d, J = 9.2 Hz), 123.9 (d, J = 3.4 Hz), 111.4(d, J = 21.4 Hz), 108.6 (d, J = 27.5 Hz), 49.3, 43.5, 37.7, 17.0. ^{19}F NMR (377 MHz, CD_3OD) δ −118.07 to −118.16 (m). HPLC-MS (ESI^+): t_R = 1.31 min; m/z = 303.1 $[M+Na]^+$, 583.1 [2 M + Na]$^+$. HRMS (ESI) m/z: $[M+Na]^+$ calcd for $C_{13}H_{13}FN_2NaO_4$ 303.0757; found 303.0765ATR-FTIR (cm^{-1}): 3337, 3096, 2972, 2929, 2611, 1885, 1769, 1715, 1610, 1555, 1492, 1456, 1420, 1330, 1308, 1280, 1258, 1203, 1161, 1123, 1096, 1064, 1004, 968, 868, 807, 746, 737, 702, 647, 623, 459.

4.1.7. 4-(2-(2-(carboxymethyl)-4-oxoazetidin-1-yl)-2-oxoethyl) benzenaminium trifluoroacetate (3)

Following GP3, compound **15** (14 mg, 0.04 mmol) yielded compound **3** as yellow oil (11 mg, 73 %). Purity by HPLC (λ = 254 nm): 95 %. ^{1}H NMR (400 MHz, CD_3OD) δ: 7.45 (d, J = 8.5 Hz, 2H), 7.32 (d, J = 1.9 Hz, 2H), 4.30 (ddd, J = 10.0, 6.9, 3.6 Hz, 1H), 4.09 (s, 2H), 3.34 (dd, J = 16.6, 8.6 Hz, 1H), 3.08 (dd, J = 16.6, 3.8 Hz, 1H), 2.96 (dd, J = 16.6, 3.8 Hz, 1H), 2.71 (dd, J = 16.6, 8.6 Hz, 1H). ^{13}C NMR (100 MHz, CD_3OD) δ: 171.4, 167.3, 132.8, 123.7, 52.7, 43.7, 43.2, 37.2. HPLC-MS (ESI^+): t_R = 1.4 min; m/z = 263[M + H-TFA]$^+$. HRMS (ESI) m/z: [M-TFA + H]$^+$ calcd for $C_{13}H_{15}N_2O_4$ 263.1026; found 263.1019. ATR-FTIR (cm^{-1}): 2957, 2925, 2865, 2619, 1791, 1681, 1516, 1434, 1410, 1370, 1330, 1309, 1275, 1201, 838, 799, 750, 723.

4.1.8. (S)-4-(2-(2-carboxypyrrolidin-1-yl)-2-oxoethyl)benzenaminium trifluoroacetate (4)

Following GP3, compound **18** (26 mg, 0.07 mmol) yielded compound **4** as yellow oil (25 mg, 99 %). Purity by HPLC (λ = 254 nm): 95 %.^{1}H NMR (600 MHz, CD_3OD) δ 7.42 (d, J = 8.2 Hz, 2H), 7.29 (d, J = 8.2 Hz, 2H), 4.45 (dd, J = 8.7, 3.3 Hz, 1H), 3.81 (q, J = 15.9 Hz, 2H), 3.66 (td, J = 6.4, 2.6 Hz, 2H), 2.26 (dqd, J = 11.4, 6.6, 2.2 Hz, 1H), 2.03 (ttd, J = 10.5, 7.4, 4.1 Hz, 3H).^{13}C NMR (151 MHz, CD_3OD) δ 175.5, 171.9, 136.7, 132.3, 132.1, 123.6, 60.4, 49.4, 49.3, 49.1, 49.0, 48.9, 48.7, 48.6, 47.9, 41.4, 30.4, 25.7. α_D^{20} = - 46 (c 1.6, MeOH). HPLC-MS (ESI^+): t_R = 1.5 min; m/z = 249 [M + H-TFA]$^+$. HRMS (ESI) m/z: [M-TFA + H]$^+$ calcd for $C_{13}H_{17}N_2O_3$ 249.1234; found 249.1230. ATR-FTIR (cm^{-1}): 3307, 2929, 1715, 1668, 1621, 1516, 1454, 1191, 1141.

4.1.9. (S)-4-((1,3-dioxotetrahydro-1H-pyrrolo[1,2-c]imidazole-2(3H)-yl) methyl)benzenaminium 2,2,2 trifluoroacetate (5)

Following GP3, compound **20** (40 mg, 0.115 mmol, 1 equiv) in anhydrous DCM (2.2 mL) in the presence of TFA (62 μL, 0.80 mmol, 7 equiv) gave compound **5** as a yellow solid in quantitative yield (30 mg, 0.115 mmol). Purity by HPLC (λ = 254 nm): 94 %. ^{1}H NMR (600 MHz, CD_3OD) δ 7.49–7.40 (m, 2H), 7.33–7.15 (m, 2H), 4.65 (d, J_{AB} = 15.1 Hz, 1H), 4.61 (d, J_{AB} = 15.1 Hz, 1H), 4.22 (dd, J = 9.4, 7.4 Hz, 1H), 3.61 (dt, J = 10.9, 7.8 Hz, 1H), 3.25 (ddd, J = 11.0, 7.9, 4.8 Hz, 1H), 2.22 (dtd, J = 12.0, 7.0, 3.7 Hz, 1H), 2.16–2.01 (m, 2H), 1.75–1.58 (m, 1H). ^{13}C NMR (151 MHz, CD_3OD) δ 175.6, 162.1, 137.6, 133.6, 130.8, 123.4, 64.8, 46.5, 42.6, 28.2, 28.0. ^{19}F NMR (377 MHz, CD_3OD) δ −77.15. HPLC-MS (ESI^+): t_R = 2.85 min; m/z = 246.2 $[M+H]^+$, 268.2 $[M+Na]^+$, 513.2 [2 M + Na]$^+$ HRMS (ESI) m/z: [M-TFA + H]$^+$ calcd for $C_{13}H_{16}N_3O$ 246.1237; found 246.1229. α_D^{20} = −22 (c 0.16, MeOH). ATR-FTIR (cm^{-1}): 2922, 2853, 1699, 1682, 1669, 1636, 1576, 1559, 1541, 1507, 1457, 1429, 1407, 1373, 1353, 1200, 1181, 1134, 1116, 1023, 970, 900, 836, 795, 765, 721, 669, 650.

4.1.10. (S)-4-(2-((1,2-dicarboxyethyl)amino)-2-oxoethyl)benzenaminium trfluororacetate (6)

Following GP3 compound **23** (27 mg, 0.073 mmol) yielded compound **6** as yellow oil (30 mg, 99 %). Purity by HPLC (λ = 254 nm): 95 %^{1}H NMR (400 MHz, CD_3OD) δ 7.47 (d, J = 8.2 Hz, 2H), 7.33 (d, J = 8.3 Hz, 2H), 4.75 (dd, J = 12.4, 6.2 Hz, 1H), 3.60 (s, 2H), 2.89–2.75 (m, 2H). ^{13}C NMR (100 MHz, CD_3OD) δ 174.1, 173.2, 135.7, 131.5, 129.3, 129.2, 129.0, 122.2, 68.7, 42.3, 36.6. $[\alpha]_D^{20}$ = 0.5 (c = 1, CD_3OH). HPLC-MS (ESI^+): t_R = 1.2 min; m/z = 267 $[M+H]^+$. HRMS (ESI) m/z: [M-TFA + H]$^+$ calcd for $C_{12}H_{15}N_2O_5$ 267.0975; found 267.0963. ATR-FTIR (cm^{-1}): 3426, 2960, 2624, 1676, 1547, 1514, 1434, 1203, 1143.

4.1.11. (S)-4-(2-((1,3-dicarboxypropyl)amino)-2-oxoethyl) benzenaminium trifluororacetate (7)

Following GP3, compound **28** (102 mg, 0.27 mmol) yielded compound **7** as yellow oil (100 mg, 99 %). Purity by HPLC (λ = 254 nm): 95 %^{1}H NMR (400 MHz, CD_3OD) δ: 7.46 (d, J = 8.1 Hz, 2H), 7.33 (d, J = 8.1 Hz, 2H), 4.43 (dd, J = 8.9, 4.9 Hz, 1H), 3.64 (s, 2H), 2.38 (t, J = 7.4 Hz, 2H), 2.19 (dt, J = 13.3, 7.8 Hz, 1H), 1.95 (dt, J = 15.0, 7.8 Hz, 1H).^{13}C NMR (100 MHz, CD_3OD) δ: 175.7, 174.5, 173.1, 137.7, 131.5, 130.1, 123.6, 52.9, 42.0, 30.6, 27.23; α_D^{20} = −8.5 (c 1, MeOH). HPLC-MS (ESI^+): t_R = 1.3 min; m/z = 281 $[M+H]^+$. HRMS (ESI) m/z: [M-TFA + H]$^+$ calcd for $C_{13}H_{17}N_2O_5$ 281.1132; found 281.1125. ATR-FTIR (cm^{-1}): 2923, 2620, 1709, 1637, 1543, 1512, 1431, 1180, 1134, 838, 796, 721.

4.1.12. (S)-4-((3-(1,2-dicarboxyethyl)ureido)methyl) benzenaminium trifluororacetate (8)

Following GP3, compound **25** (35 mg, 0.0926 mmol) yielded compound **8** as yellow oil (22 mg, 84 %). Purity by HPLC (λ = 254 nm): 95 %^{1}H NMR (400 MHz CD_3OD) δ 7.45 (d, J = 7.7 Hz, 2H), 7.29 (d, J = 7.1 Hz, 2H), 4.61 (s, 1H), 4.38 (s, 2H), 2.84 (m, 2H). ^{13}C NMR (100 MHz, CD_3OD) δ 160.4, 141.0, 130.5, 129.6, 123.0, 55.1, 43.9, 37.9, 30.7. α_D^{20} = 4.6 (c 1, MeOH). HPLC-MS(ESI^+): t_R = 1.3 min; m/z = 282 $[M+H]^+$ HRMS (ESI) m/z: [M-TFA + H]$^+$ calcd for $C_{12}H_{16}N_3O_5$ 282.1084; found 282.1076. ATR-FTIR (cm^{-1}): 3369, 2926, 2615, 1713, 1672, 1652,1567, 1515, 1199, 1141, 842.

4.1.13. 4-(2-((2-carboxyethyl)amino)-2-oxoethyl)benzenaminium trfluororacetate (9)

Following GP3, compound **31** (22 mg, 0.07 mmol) yielded compound **9** as yellow oil (24 mg, 99 %). Purity by HPLC (λ = 254 nm): 95 %. ^{1}H NMR (400 MHz, CD_3OD) δ: 7.43 (d, J = 8.0 Hz, 2H), 7.33 (d, J = 8.0 Hz, 2H), 3.55 (s, 2H), 3.43 (t, J = 6.7 Hz, 2H), 2.50 (t, J = 6.6 Hz, 2H). ^{13}C NMR (100 MHz, CD_3OD) δ:175.4, 138.5, 132.1, 130.9, 124.3, 43.1, 36.8, 34.7. HPLC-MS (ESI^+): t_Rr_t = 1.5 min; m/z = 223 [M + H-TFA]$^+$. HRMS (ESI) m/z: [M-TFA + H]$^+$ calcd for $C_{11}H_{15}N_2O_3$ 223.1077; found 223.1069. ATR-FTIR (cm^{-1}): 1675, 1514, 1200, 1139, 723.

4.1.14. 3-(3-(4-aminobenzyl)ureido)propanoic acid (10)

Following GP2, **32** (50 mg, 0.108 mmol, 1 equiv) was reacted in 4.5 mL of THF/MeOH with Pd/C (10 mg, 20 % wt) yielding **10** (24 mg, 0.101 mmol) as a pale yellow solid in 94 % yield. Purity by HPLC (λ = 254 nm): 94.8 %.^{1}H NMR (600 MHz, CD_3OD) δ 7.05–7.00 (m, 2H), 6.71–6.65 (m, 2H), 4.15 (s, 2H), 3.37 (t, J = 6.5 Hz, 2H), 2.42 (t, J = 6.5 Hz, 2H). ^{13}C NMR (151 MHz, CD_3OD) δ 177.8, 161.0, 147.6, 130.7, 129.4, 116.7, 44.5, 37.5, 37.2; HPLC-MS (ESI^+): t_R = 0.99 min; m/z = 238 $[M+H]^+$, 260 $[M+Na]^+$ HRMS (ESI) m/z: [M-TFA + H]$^+$ calcd for

$C_{11}H_{16}N_3O_3$ 238.1186; found 238.1177. ATR-FTIR (cm^{-1}): 767, 829, 903,1017, 1052, 1155, 1235, 1315, 1366, 1394, 1410, 1522, 1559, 1595, 1617, 1699 2929, 2976, 3345.

4.1.15. Benzyl 2-(4-oxo-1-((2-(trifluoromethyl)phenyl)carbamoyl) azetidin-2-yl)acetate (12)

In a round bottom flask under nitrogen atmosphere, anhydrous TEA (160 μL, 1.14 mmol, 5 equiv) was added to a solution of compound **11** (50 mg, 0.23 mmol, 1 equiv.) in anhydrous DCM (2 mL). After 20 min, 1-isocyanato-2-(trifluoromethyl) benzene (7 equiv), dissolved in 3 mL of DCM, was added dropwise. The reaction was left at room temperature overnight and monitored by TLC. At completion, the reaction was quenched with a saturated aqueous solution of NH_4Cl and extracted with DCM (3x10 mL). The collected organic layers were dried on Na_2SO_4, filtered and the solvent removed under reduced pressure. The crude was purified by flash chromatography on silica gel (15:85 EtOAc: Cyclohexane), giving compound **12** as a white solid in 55 % yield (51 mg, 0.126 mmol). ^{1}H NMR (400 MHz, $CDCl_3$) δ 8.80 (bs, 1H), 8.01 (d, J = 8.4 Hz, 1H), 7.54 (d, J = 8.4 Hz, 1H), 7.51–7.38 (m, 1H), 7.31–7.20 (m, 5H), 7.19–7.10 (m, 1H), 5.10 (d, J = 12.9 Hz, 2H), 5.06 (d, J = 12.9 Hz, 2H), 4.48–4.28 (m, 1H), 3.34–3.12 (m, 2H), 2.88 (ddd, J = 16.4, 3.1, 1.0 Hz, 1H), 2.72 (dd, J = 16.5, 8.8 Hz, 1H). ^{19}F NMR (377 MHz, $CDCl_3$) δ −61.14 (s). ^{13}C NMR (100 MHz, $CDCl_3$) δ 169.7, 166.5, 147.9, 135.5, 134.6 (q, J = 1.9 Hz), 132.9, 128.8, 128.6, 128.5, 126.4 (q, J = 5.3 Hz), 124.6, 124.0, 123.5 (q, J = 271.3 Hz), 120.7 (t, J = 30.1 Hz), 67.2, 47.8, 43.0, 37.1. HPLC-MS (ESI^+): t_R = 10.3 min; m/z = 407.4 $[M+H]^+$, 429.4 $[M+Na]^+$. ATR-FTIR (cm^{-1}): 3341, 3065, 2960, 2447, 2342, 1776,1731, 1618, 1596, 1555, 1458, 1322, 1287, 1246, 1172, 1118, 1064, 1036, 765, 749, 699, 652, 625.

4.1.16. Benzyl 2-(1-((5-fluoro-2-methylphenyl)carbamoyl)-4-oxoazetidin-2-yl)acetate (13)

In a round bottom flask under nitrogen atmosphere, anhydrous TEA (160 μL, 1.14 mmol, 5 equiv) was added to a solution of compound **11** (50 mg, 0.23 mmol, 1 equiv) in anhydrous DCM (2 mL). After 20 min, 4-fluoro-2-isocyanato-1-methylbenzene (7 equiv), dissolved in 3 mL of DCM, was added dropwise. The reaction was left at room temperature overnight and monitored by TLC. At completion, the reaction was quenched with a saturated aqueous solution of NH_4Cl and extracted with DCM (3x10 mL). The collected organic layers were dried on Na_2SO_4, filtered and the solvent removed under reduced pressure. The crude was purified by flash chromatography on silica gel (15:85 EtOAc: Cyclohexane), giving compound **13** as a white solid in 66 % yield (56 mg, 0.151 mmol).

^{1}H NMR (400 MHz, $CDCl_3$) δ 8.42 (s, 1H), 7.75 (dd, J = 11.0, 2.7 Hz, 1H), 7.30–7.21 (m, 5H), 7.02 (dd, J = 8.4, 6.3 Hz, 1H), 6.65 (td, J = 8.2, 2.7 Hz, 1H), 5.08 (d, J_{AB} = 12.7 Hz, 1H), 5.07 (d, J_{AB} = 12.8 Hz, 1H), 4.45–4.35 (m, 1H), 3.27 (ddd, J = 16.1, 10.8, 4.9 Hz, 2H), 2.94–2.84 (m, 1H), 2.75 (dd, J = 16.5, 8.6 Hz, 1H), 2.16 (s, 3H). ^{19}F NMR (377 MHz, $CDCl_3$) δ −114.43 to −115.42 (m). ^{13}C NMR (100 MHz, $CDCl_3$) δ 169.8, 166.9, 161.5 (d, J = 242.4 Hz), 147.7, 136.6 (d, J = 11.2 Hz), 135.5, 131.2 (d, J = 9.1 Hz), 128.8, 128.6, 128.5, 122.0 (d, J = 3.4 Hz), 110.7 (d, J = 21.4 Hz), 107.9 (d, J = 27.4 Hz), 67.0, 47.8, 42.8, 37.0, 17.1. HPLC-MS (ESI^+): t_R = 10.3 min; m/z = 371.4 $[M+H]^+$, 393.4 $[M+Na]^+$ ATR-FTIR (cm^{-1}): 3336, 3310, 3034, 2929, 1768, 1733. 1718, 1609, 1533, 1493, 1456, 1390, 1333, 1310, 1280, 1258, 1175, 1161, 1126, 1063, 1003, 967, 868, 805, 747, 699, 622, 426.

4.1.17. Benzyl 2-(1-(2-(4-((tert-butoxycarbonyl)amino)phenyl)acetyl)-4-oxoazetidin-2-yl)acetate (14)

To a solution of 2-(4-((*tert*-butoxycarbonyl)amino)phenyl)acetic acid (114 mg, 0.46 mmol, 1 equiv) in 4 mL of DCM, under a nitrogen atmosphere at 0 °C, HBTU (383 mg, 0.92 mmol, 2 equiv), DIPEA (320 μL, 1.84 mmol, 4 equiv) and compound **11** (100 mg, 0.46, 1 equiv.) were added. The reaction was left under stirring overnight. At completion (TLC monitoring) the mixture was quenched with NH_4Cl and extracted with EtOAc. The organic layer was dried over Na_2SO_4, concentrated in vacuum, and purified by flash chromatography (Cyclohexane:EtOAc = 7:3). Compound **14** (54 mg; 26 %) was obtained as colourless oil. ^{1}H NMR (400 MHz, $CDCl_3$) δ: 7.40–7.27 (m, 7H), 7.21 (d, J = 8.5 Hz, 2H), 6.43 (bs, 1H), 5.10 (d, J = 1.4 Hz, 2H), 4.34–4.27 (m, 1H), 3.92 (s, 2H), 3.27 (dd, J = 9.4, 5.2 Hz, 1H), 3.23 (dd, J = 9.3, 5.2 Hz, 1H), 2.85 (dd, J = 16.6, 3.4 Hz, 1H), 2.64 (dd, J = 16.4, 8.8 Hz, 1H), 1.51 (s, 9). ^{13}C NMR (100 MHz, $CDCl_3$) δ: 170.2, 169.6, 164.8, 153.2, 138.1, 135.9, 130.6, 129.2, 129.0, 128.9, 128.1, 119.2, 81.1, 67.3, 47.2, 43.1, 42.6, 37.2, 28.9. HPLC-MS (ESI^+): t_R = 10.7 min; m/z = 470 $[M + NH_4]^+$. ATR-FTIR (cm^{-1}): 3350, 3113, 3062, 3034, 2977, 2930, 2854, 1791, 1702, 1613, 1595, 1525, 1455, 1414, 1366, 1319, 1266, 1235, 1161, 1053, 1027, 1018, 902, 838, 808, 736, 698.

4.1.18. 2-(1-(2-(4-((tert-butoxycarbonyl)amino)phenyl)acetyl)-4-oxoazetidin-2-yl)acetic acid (15)

Following GP2, compound **14** (40 mg, 0.09 mmol) yielded compound **15** as white solid (34 mg, 99 %). ^{1}H NMR (400 MHz, CD_3OD) δ: 7.33 (d, J = 8.2 Hz, 2H), 7.18 (d, J = 8.3 Hz, 2H), 4.31–4.23 (m, 1H), 3.94 (d, J = 3.5 Hz, 2H), 3.27 (dd, J = 16.4, 8.8 Hz, 1H), 3.09 (dd, J = 16.5, 3.5 Hz, 1H), 2.93 (dd, J = 16.5, 3.2 Hz, 1H), 2.65 (dd, J = 16.4, 8.8 Hz, 1H), 1.51 (s, 9H). ^{13}C NMR (100 MHz, CD_3OD) δ: 171.6, 167.2, 156.0, 140.1, 131.4, 129.6, 120.4, 82.0, 55.5, 43.8, 43.4, 37.2, 29.3. HPLC-MS (ESI^+): t_R = 7.4 min; m/z = 380 $[M + NH_4]^+$. ATR-FTIR (cm^{-1}): 3341, 3057, 2979, 2932, 1790, 1713, 1613, 1596, 1525, 1415, 1392, 1367, 1319, 1268, 1236, 1160, 1056, 1028, 984, 901, 862, 809, 772, 737, 703.

4.1.19. Benzyl (2-(4-((tert-butoxycarbonyl)amino)phenyl)acetyl)-L-prolinate (17)

To a solution of enantiopure L-proline-benzyl ester TFA salt **16** (65 mg, 0.20 mmol, 1 equiv) in 1.8 mL of DCM, under nitrogen atmosphere, 2-(4-((*tert*-butoxycarbonyl)amino)phenyl)acetic acid (51 mg, 0.20 mmol, 1 equiv) and DMAP (12 mg, 0.1 mmol, 0.5 equiv.) were added. The mixture was then cooled to 0 °C, and DCC (45 mg, 0.22 mmol, 1.1 equiv) was added; the system was allowed to reach room temperature in 15 min and left under stirring overnight. After 24 h (TLC monitoring), the reaction mixture was filtered washing with DCM and evaporated. The crude was suspended in EtOAc at 0 °C, and the solid residual dicyclohexylurea was eliminated by filtration. The organic layer was concentrated in vacuum and purified by flash chromatography (Cyclohexane:EtOAc = 6:4). Compound **17** (38 mg; 43 %) was obtained as colourless oil. ^{1}H NMR (400 MHz, $CDCl_3$) δ 7.41–7.23 (m, 7H), 7.18 (d, J = 8.9 Hz, 2H), 6.50 (bs, 1H), 5.18 (d, J_{AB} = 13.1 Hz, 1H), 5.13 (d, J_{AB} = 12.9 Hz, 1H), 4.55 (dd, J = 8.7, 3.5 Hz, 1H), 3.64 (s, 2H), 3.58 (td, J = 9.0, 6.1 Hz, 1H), 3.50–3.42 (m, 1H), 2.27–2.06 (m, 1H), 2.01–1.81 (m, 3H), 1.51 (d, J = 2.2 Hz, 9H). ^{13}C NMR (100 MHz, $CDCl_3$) δ 172.2, 171.3, 152.9, 137.8, 135.8, 130.0, 129.2, 128.7, 128.5, 128.3, 119.1, 80.6, 66.6, 43.1, 35.2, 34.1, 28.4. α_D^{20} = 39.5 (*c* 1, DCM). HPLC-MS (ESI^+): t_R = 10.1 min; m/z = 439 $[M+H]^+$. ATR-FTIR (cm^{-1}): 3045, 1728, 1645, 1265, 738, 705.

4.1.20. (2-(4-((tert-butoxycarbonyl)amino)phenyl)acetyl)-L-proline (18)

Following GP2, compound **17** (38 mg, 0.09 mmol) yielded compound **18** as white solid (26 mg, 83 %).^{1}H NMR (400 MHz, CD_3OD) δ 7.34 (t, J = 6.3 Hz, 3H), 7.25–7.08 (m, 3H), 4.43 (d, J = 8.4 Hz, 1H), 3.68 (s, 2H), 3.59 (tt, J = 11.3, 5.7 Hz, 2H), 2.23 (d, J = 8.1 Hz, 1H), 1.98 (q, J = 9.2 Hz, 3H), 1.51 (s, 9H). ^{13}C NMR (100 MHz, CD_3OD) δ: 155.1, 139.2, 130.7, 130.2, 119.8, 80.6, 42.9, 36.4, 34.5, 28.5. α_D^{20} = - 129 (*c* 1.2, MeOH). HPLC-MS (ESI^+): t_R = 6.3 min; m/z = 349 $[M+H]^+$. ATR-FTIR (cm^{-1}): 2978, 2931, 1720, 1600, 1526, 1451, 1238, 1161, 1028.

4.1.21. Benzyl ((4-((tert-butoxycarbonyl)amino)benzyl)carbamoyl)-L-prolinate (19)

In a round bottom flask under nitrogen atmosphere, anhydrous TEA

(74 μL, 0.526 mmol, 2 equiv) was added to a solution of proline benzylester PTSA salt (**16**) (84 mg, 0.263 mmol, 1 equiv) in anhydrous DCM (5.5 mL). After 20 min, *tert*-butyl(4-(isocyanatomethyl)phenyl)carbamate (2 equiv), dissolved in 3 mL of DCM, was added dropwise. The reaction was left at room temperature overnight and monitored by TLC. At completion, the reaction was quenched with a saturated aqueous solution of NH_4Cl and extracted with DCM (3x10 mL). The collected organic layers were dried on Na_2SO_4, filtered and the solvent removed under reduced pressure. The crude was purified by flash chromatography on silica gel (30:70 EtOAc: Cyclohexane), giving compound **19** as a white solid in 36 % yield (43 mg, 0.095 mmol). ^{1}H NMR (600 MHz, $CDCl_3$) δ 7.38–7.24 (m, 6H), 7.22–7.16 (m, 2H), 6.67 (bs, 1H), 5.18 (d, J_{AB} = 12.4 Hz, 1H), 5.10 (d, J_{AB} = 12.4 Hz, 1H), 4.74 (t, J = 5.6 Hz, 1H), 4.49 (dd, J = 8.6, 2.8 Hz, 1H), 4.36 (dd, J = 14.5, 5.7 Hz, 1H), 4.30 (dd, J = 14.6, 5.4 Hz, 1H), 3.44 (td, J = 8.4, 4.3 Hz, 1H), 3.37–3.29 (m, 1H), 2.20–2.09 (m, 1H), 2.06–1.96 (m, 2H), 1.94 (ddp, J = 11.4, 7.8, 3.9 Hz, 1H), 1.50 (s, 9H). ^{13}C NMR (151 MHz, $CDCl_3$) δ 173.1, 156.5, 152.9, 137.7, 135.8, 134.1, 128.6, 128.5, 128.3, 128.2, 118.9, 80.5, 66.9, 59.2, 45.9, 44.3, 29.8, 28.4, 24.5. HPLC-MS (ESI$^+$): t_R = 8.58 min; m/z = 454 $[M+H]^+$, 476 $[M+Na]^+$, 907 [2 M + H]$^+$. ATR-FTIR (cm^{-1}): 3159, 2924, 2853, 2359, 2331, 1699, 1683, 1670, 1560, 1541, 1515, 1457, 1431, 1410, 1335, 1137, 1088, 1025, 971, 920, 837, 796, 768, 723. Melting point: 211 °C. α_D^{20} = +21 (*c* 0.08, CH_2Cl_2).

4.1.22. ((4-((tert-butoxycarbonyl)amino)benzyl)carbamoyl)-L-proline (20)

Following GP2, compound **19** (54 mg, 0.119 mmol, 1 equiv) in 5 mL of THF:MeOH, in the presence of Pd/C (20 % w/w) gave compound **20** in 92 % yield (23 mg, 0.109 mmol) as a white solid. Mixture of rotamers observed on NMR analysis at 25 °C (Major:Minor = 1:0.18).

^{1}H NMR (600 MHz, CD_3OD) δ 7.33 (m, 2H$_{Major}$, 2H$_{Minor}$), 7.21 (m, 2H$_{Major}$, 2H $_{Minor}$), 4.54 (d, J_{AB} = 14.8 Hz, 1H$_{Minor}$), 4.50 (d, J_{AB} = 14.8 Hz, 1H$_{Minor}$), 4.39 (dd, J = 8.6, 2.9 Hz, 1H$_{Major}$), 4.32 (d, J_{AB} = 15.2 Hz, 1H$_{Major}$), 4.26 (d, J_{AB} = 15.3 Hz, 1H$_{Major}$), 4.17 (dd, J = 9.3, 7.4 Hz, 1H$_{Minor}$), 3.59 (dt, J = 11.1, 7.8 Hz, 1H$_{Minor}$), 3.49 (td, J = 8.2, 4.5 Hz, 1H$_{Major}$), 3.38 (q, J = 7.9 Hz, 1H$_{Major}$), 3.22 (ddd, J = 11.1, 7.9, 4.7 Hz, 1H$_{Minor}$), 2.27–2.15 (m, 1H$_{Major}$, 1H$_{Minor}$), 2.10–1.92 (m, 3H$_{Major}$, 3H$_{Minor}$), 1.51 (s, 9H$_{Major}$, 9H$_{Minor}$).

^{13}C NMR (151 MHz, CD_3OD) δ 176.9 (Major), 175.6 (Minor), 162.3 (Minor), 159.1 (Major), 155.32 (Major), 155.2 (Minor), 140.2 (Minor), 139.2 (Major), 135.7 (Major), 131.8 (Minor), 129.7 (Minor), 128.7 (Major), 119.8 (Minor, Major), 80.7 (Minor, Major), 64.7 (Minor), 60.5 (Major), 47.0 (Major), 46.4 (Minor), 44.5 (Major), 42.9 (Minor), 30.9 (Minor), 30.8 (Major), 28.71 (Major), 28.7 (Minor), 25.3 (Major, Minor). ATR-FTIR (cm^{-1}) = 2963, 2925, 2364, 1699, 1634, 1615, 1597, 1522, 1474, 1457, 1410, 1392, 1366, 1313, 1457, 1410, 1392, 1366, 1313, 1233, 1153, 1051, 1015, 967, 902, 874, 795, 767, 736; α_D^{20} = - 12 (*c* 0.39, CH_3OH).

4.1.23. Dibenzyl L-aspartate p-toluensulfonic acid (21)

Following GP1, commercially available enantiopure L-aspartic acid (100 mg, 0,75 mmol) yielded compound **21** as white solid (240 mg, 66 %). The spectroscopic data matched those reported in the literature [81].

4.1.24. Dibenzyl L-glutamate p-toluensulfonic acid (26)

Following GP1, commercially available enantiopure L-glutamic acid (100 mg, 0.68 mmol) yielded compound **26** as white solid (240 mg, 70 %). The spectroscopic data matched those reported in the literature [84].

4.1.25. β-Alanine benzyl ester p-toluenesulfonate salt (29)

Following GP1, β-Alanine (1 g, 11 mmol,1 equiv) and benzyl alcohol (2 mL, 22 mmol, 2 equiv) yielded compound **29** as white solid (2.51 g, 7.15 mmol, 65 %). The spectroscopic data matched those reported in the literature [85].

4.1.26. Dibenzyl (2-(4-((tert-butoxycarbonyl)amino)phenyl)acetyl)-L-aspartate (22)

Following GP4, compound **21** (55 mg, 0.11 mmol) and 2-(4-((*tert*-butoxycarbonyl)amino)phenyl)acetic acid (28 mg, 0.11 mmol) yielded compound **22** as white solid (40 mg, 67 %). ^{1}H NMR (400 MHz, $CDCl_3$) δ 7.38–7.15 (m, 11H), 7.08 (d, J = 8.5 Hz, 2H), 6.52 (s, 1H), 6.43 (d, J = 8.0 Hz, 1H), 5.06 (s, 2H), 4.99 (s, 2H), 4.89–4.83 (m, 1H), 3.47 (s, 2H), 3.01 (dd, J = 17.1, 4.6 Hz, 1H), 2.84 (dd, J = 17.1, 4.6 Hz, 1H), 1.50 (s, 9H). ^{13}C NMR (100 MHz, $CDCl_3$) δ 171.4, 171.0, 170.9, 153.3, 138.2, 135.9, 135.6, 130.4, 129.2, 129.1, 129.1, 129.0, 128.9, 128.9, 128.8, 119.4, 81.2, 68.1, 67.3, 49.3, 43.3, 36.8, 28.9. $[\alpha]_D^{25}$ = 11.2 (c = 1, CH_2Cl_2). HPLC-MS (ESI$^+$): t_R = 10.7 min; m/z = 547 $[M+H]^+$. ATR-FTIR (cm^{-1}): 3306, 3189, 3089, 3064, 3034, 2977, 2932, 1726, 1659, 1524, 1235, 1162, 1052, 737.

4.1.27. Dibenzyl (2-(4-((tert-butoxycarbonyl)amino)phenyl)acetyl)-L-glutamate (27)

Following GP4, compound **26** (210 mg, 0.48 mmol) and 2-(4-((*tert*-butoxycarbonyl)amino)phenyl)acetic acid (122 mg, 0.48 mmol) yielded compound **27** as white solid (157 mg, 56 %). ^{1}H NMR (400 MHz, $CDCl_3$) δ 7.39–7.26 (m, 12H), 7.14 (d, J = 8.3 Hz, 2H), 6.54 (bs, 1H), 6.13 (d, J = 7.8 Hz, 1H), 5.11 (s, 2H), 5.05 (s,2H), 4.68–4.61 (m, 1H), 3.50 (s, 2H), 2.42–2.26 (m, 2H), 2.19 (td, J = 13.3, 6.7 Hz, 1H), 1.94 (td, J = 14.2, 7.8 Hz, 1H), 1.52 (s, 9H). ^{13}C NMR (100 MHz, $CDCl_3$) δ 172.8, 171.8, 171.6, 153.1, 138.1, 136.0, 135.4, 130.3, 129.0, 128.9, 128.9, 128.8, 128.6, 128.6, 128.6, 119.3, 81.1, 67.4, 66.5, 52.1, 43.1, 30.5, 28.7, 27.4. α_D^{20} = −1.7 (*c* 1, DCM). HPLC-MS (ESI$^+$): t_R = 9.8 min; m/z = 561 $[M+H]^+$. ATR-FTIR (cm^{-1}): 3342, 1728, 1696, 1648, 1521, 1240, 1154, 1056, 807, 734, 695.

4.1.28. (2-(4-((tert-butoxycarbonyl)amino)phenyl)acetyl)-L-aspartic acid (23)

Following GP2 compound **22** (40 mg, 0.073 mmol) yielded compound **23** as waxy solid (27 mg, 99 %). ^{1}H NMR (400 MHz, CD_3OD) δ 7.34 (d, J = 8.2 Hz, 2H), 7.19 (d, J = 8.4 Hz, 2H), 4.79–4.68 (m, 1H), 3.51 (s, 2H), 2.91–2.75 (m, 2H), 1.51 (s, 9H). ^{13}C NMR (100 MHz, CD_3OD) δ 174.0, 155.3, 139.4, 130.6, 119.9, 80.8, 42.8, 36.9, 28.7; α_D^{20} = 5.3 (*c* 1, MeOH). HPLC-MS (ESI$^+$): t_R = 4.6 mi; m/z = 311$[M+H]^+$. ATR-FTIR (cm^{-1}): 3310, 2957, 2925, 2855, 1719, 1654, 1648, 1524, 1458, 1318, 1233.

4.1.29. (2-(4-((tert-butoxycarbonyl)amino)phenyl)acetyl)L-glutamic acid (28)

Following GP2, compound **27** (150 mg, 0.27 mmol) yielded compound **28** as waxy solid (102 mg, 99 %). ^{1}H NMR (400 MHz, CD_3OD) δ 7.34 (d, J = 8.1 Hz, 2H), 7.20 (d, J = 8.2 Hz, 2H), 4.43 (dd, J = 8.6, 4.9 Hz, 1H), 3.51 (s, 2H), 2.37 (t, J = 7.4 Hz, 2H), 2.24–2.12 (m, 1H), 2.00–1.88 (m, 1H), 1.51 (s, 9H).^{13}C NMR (100 MHz, CD_3OD) δ 176.6, 174.3, 155.6, 139.4, 139.4, 130.9, 130.5, 119.9, 81.4, 53.2, 42.9, 31.2, 28.7, 27.9; α_D^{20} = −8 (*c* 1, MeOH). HPLC-MS (ESI$^+$): t_R = 3.9 min; m/z = 381 $[M+H]^+$. ATR-FTIR (cm^{-1}): 2922, 2256, 2113, 1990, 1706, 1524, 1415, 1237, 1160, 814.

4.1.30. Dibenzyl ((4-((tert-butoxycarbonyl)amino)benzyl)carbamoyl)-L-aspartate (24)

To a solution of compound **21** (95 mg, 0.19 mmol, 1 equiv) and TEA (53 μL, 0.38 mmol, 2 equiv) in 1.2 mL of DCM, under a nitrogen atmosphere, the previously synthesized *tert*-butyl(4-(isocyanatomethyl) phenyl)carbamate was added, and the reaction was left at rt overnight. At completion (TLC monitoring) the mixture was quenched with NH_4Cl and extracted with DCM. The organic layer was dried over Na_2SO_4, concentrated in vacuum, and purified by flash chromatography (Cyclohexane:AcOEt from 7:3 to 6:4). Compound **24** (50 mg; 47 %) was

obtained as colourless oil. ^{1}H NMR (400 MHz, $CDCl_3$) δ 7.33–7.28 (m, 7H), 7.27–7.22 (m, 2H), 7.15 (d, J = 8.4 Hz, 2H), 6.51 (bs, 1H), 5.07 (s, 2H), 5.00 (d, J = 2.9 Hz, 2H), 4.84 (t, J = 4.3 Hz, 1H), 4.24 (s, 2H), 3.05 (dd, J = 17.1, 4.6 Hz, 1H), 2.88 (dd, J = 17.0, 4.6 Hz, 1H), 1.50 (s, 9H).^{13}C NMR (100 MHz, $CDCl_3$) δ 172.3, 171.7, 157.8, 153.6, 138.1, 136.4, 134.4, 129.1, 129.1, 128.9, 128.8, 128.8, 128.7, 119.3, 67.9, 67.2, 50.2, 44.6, 37.7, 28.9; α_D^{20} = 4.7 (c 1, DCM). HPLC-MS (ESI$^+$): t_R = 10.5 min; m/z = 561 $[M+H]^+$. ATR-FTIR (cm^{-1}): 3360, 2978, 2931, 1729, 1643, 1597, 1526, 1456, 1413, 1356, 1316, 1237, 1163, 1053.

4.1.31. ((4-((tert-butoxycarbonyl)amino)benzyl)carbamoyl)-L-aspartic acid (25)

Following GP2, compound **24** (50 mg, 0.09 mmol) yielded compound **25** as waxy solid (35 mg, 98 %). ^{1}H NMR (400 MHz, CD_3OD) δ 8.82 (s, 1H), 7.33 (d, J = 8.0 Hz, 2H), 7.19 (d, J = 8.3 Hz, 2H), 4.65 (s, 1H), 4.26 (s, 2H), 2.84 (d, J = 16.7 Hz, 2H), 1.51 (s, 9H).^{13}C NMR (100 MHz, CD_3OD) δ 155.8, 139.3, 135.1, 130.6, 128.6, 119.7, 80.6, 44.2, 38.3, 28.6; α_D^{20} = 12.5 (c 1, MeOH). HPLC-MS (ESI$^+$): t_R = 4.4 min; m/z = 382 $[M+H]^+$. ATR-FTIR (cm^{-1}): 3339, 2979, 2931, 1714, 1644, 1616, 1598, 1529, 1414, 1393, 1368, 1316, 1242, 1162, 1056.

4.1.32. Benzyl 3-(2-(4-((tert-butoxycarbonyl)amino)phenyl)acetamido) propanoate (30)

Following GP4, 2-(4-((*tert*-butoxycarbonyl)amino)phenyl)acetic acid (36 mg, 0.14 mmol) and compound **29** (50 mg, 0.14 mmol) yielded compound **30** as white solid (42 mg, 73 %). ^{1}H NMR (400 MHz, $CDCl_3$) δ 7.41–7.24 (m, 7H), 7.14–7.08 (m, 2H), 6.56 (bs, 1H), 5.93 (bs, 1H), 5.08 (s, 2H), 3.51–3.44 (m, 4H), 2.58–2.50 (m, 2H), 1.50 (s, 9H). ^{13}C NMR (100 MHz, $CDCl_3$) δ 172.2, 171.3, 152.9, 137.8, 135.7, 129.9, 129.2, 128.7, 128.5, 128.3, 119.1, 80.7, 66.6, 43.1, 35.2, 34.1, 28.4. HPLC-MS (ESI$^+$): t_R = 9.3 min; m/z = 413 $[M+H]^+$. ATR-FTIR (cm^{-1}): 3189, 2978, 2932, 1726, 1654, 1597, 1526, 1240, 1164, 1054, 737.

4.1.33. 3-(2-(4-((tert-butoxycarbonyl)amino)phenyl)acetamido) propanoic acid (31)

Following GP2, compound **30** (42 mg, 0.10 mmol) yielded compound **31** as white solid (22 mg, 68 %). ^{1}H NMR (400 MHz, CD_3OD) δ 7.33 (d, J = 8.0 Hz, 2H), 7.16 (d, J = 8.0 Hz, 2H), 3.47–3.34 (m, 4H), 2.53–2.39 (m, 2H), 1.51 (s, 9H). ^{13}C NMR (100 MHz, CD_3OD) δ 155.1, 139.2, 130.7, 130.2, 119.8, 80.6, 42.9, 36.4, 34.5, 28.5. HPLC-MS (ESI$^+$): t_R = 4.6 min; m/z = 340 $[M + NH_4]^+$. ATR-FTIR (cm^{-1}) 2980, 1714, 1651, 1521, 1392, 1239, 1162, 738.

4.1.34. Benzyl 3-(3-(4-(((benzyloxy)carbonyl)amino)benzyl)ureido) propanoate (32)

In a round bottom flask under nitrogen atmosphere, anhydrous TEA (55 μL, 0.390 mmol, 2 equiv.) was added to a solution of compound **29** (68.4 mg, 0.195 mmol, 1 equiv.) in anhydrous DCM (2 mL). After 20 min, benzyl (4-(isocyanatomethyl)phenyl)carbamate (110 mg, 0.390 mmol, 2 equiv.), dissolved in 4 mL of DCM, was added dropwise. The reaction was left at room temperature overnight and monitored by TLC. At completion, the reaction was quenched with a saturated aqueous solution of NH_4Cl and extracted with DCM (3x10 mL). The collected organic layers were dried on Na_2SO_4, filtered and the solvent removed under reduced pressure. The crude was purified by flash chromatography on silica gel (50:50 to 60:40 EtOAc: Cyclohexane), giving compound **32** as a white solid in 76 % yield (68 mg, 0.148 mmol). ^{1}H NMR (600 MHz, Acetone-d6) δ 8.70 (s, 1H), 7.49 (d, J = 8.1 Hz, 2H), 7.42 (d, J = 7.3 Hz, 2H), 7.40–7.28 (m, 7H), 7.25–7.19 (m, 2H), 5.91 (t, J = 6.0 Hz, 1H), 5.67 (t, J = 6.1 Hz, 1H), 5.16 (s, 2H), 5.11 (s, 2H), 4.27 (d, J = 5.9 Hz, 2H), 3.43 (q, J = 6.3 Hz, 2H), 2.57 (t, J = 6.4 Hz, 2H). ^{13}C NMR (151 MHz, Acetone-d6) δ 172.7, 158.8, 154.4, 138.8, 137.9, 137.5, 136.2, 129.3, 129.3, 128.9, 128.8, 128.8, 128.7, 119.1, 66.8, 66.5, 43.9, 36.7, 35.9. HPLC-MS (ESI$^+$): t_R = 8,15 min; m/z = 462 $[M+H]^+$, 484 $[M+Na]^+$. ATR-FTIR (cm^{-1}): 3336, 3038, 2926, 1726, 1702, 1618, 1560, 1523, 1357, 1306, 1284, 1239, 1165, 1060, 964, 909, 839, 740, 699.

4.2. Pharmacology

4.2.1. Cell culture

Jurkat E6.1 (human acute T cell leukaemia cell line, expressing $\alpha_4\beta_1$ integrin), K562 (human erythroleukemic cells, expressing $\alpha_5\beta_1$ integrin) and HL-60 (human promyelocytic leukaemia cell line, expressing $\alpha_M\beta_2$ integrin) cells were grown in RPMI-1640 (Life Technologies, Carlsbad, CA, USA) supplemented with 1 % L-glutamine and 10 % FBS (foetal bovine serum, Life Technologies). Cells were kept at 37 °C under 5 % CO_2 humified atmosphere. 48 h before experiments, K562 cells were treated with 65 nM PMA (phorbol 12-myristate 13-acetate, Sigma-Aldrich, Milan, Italy) to induce cell differentiation and to increase $\alpha_5\beta_1$ integrin expression on the cell surface. All cell lines were obtained from American Type Culture Collection (ATCC, Rockville, MD, USA). The cell lines employed in this study are considered useful *in vitro* models to investigate potential integrin ligand effects on cell adhesion and integrin-mediated intracellular signal transduction [42,43,and86]].

4.2.2. LDV-FITC competitive binding assay

The affinity for $\alpha_4\beta_1$ integrin was determined by LDV-FITC competitive binding assay as previously reported [59]. Jurkat E6.1 cells (50,000 cells/sample) were suspended in 0.1 % BSA in HEPES Buffer (NaCl 110 mM; KCl 10 mM; Glucose 10 mM; $MgCl_2$ 1 mM; $CaCl_2$ 1.5 mM; HEPES 30 mM; pH 7.4; 0.1 % BSA w/v) and pre-incubated with increasing concentrations of the compounds (10^{-11} – 10^{-5} M) or vehicle (methanol) for 30 min at room temperature. Afterward, LDV-FITC (5 μM, Tocris Bioscience™) was added to the cells-compound suspension and samples were incubated for 30 min at room temperature in the dark. At the end of the incubation, cells were washed with 0.1 % BSA in HEPES Buffer and plated in a black 96-well microplate (Corning Costar). FITC fluorescence intensity was measured (Ex492 nm/Em517 nm) using an EnSpire Multimode Plate Reader (PerkinElmer, Waltham, MA, USA). The data were represented by a graph showing LDV-FITC specific binding versus competitor concentrations, and data were analysed as one-site competition equation. The equilibrium dissociation constant, K_i, was calculated using the Cheng-Prusoff equation.

4.2.3. Cell adhesion assays

The cell adhesion assays were done as previously described [42,87,88]. Briefly, for adhesion assay on Jurkat E6.1, black 96-well plates (Corning Costar) were coated by passive adsorption with FN (fibronectin; 10 μg/mL) or VCAM-1 (vascular cell adhesion molecule-1; 2 μg/mL) overnight at 4 °C. The following day plates were incubated for 30 min at 37 °C with blocking solution (1 % BSA in HBSS; Hank's Balanced Salt Solution, Life Technologies), to avoid unspecific binding. Cells were stained for 30 min at 37 °C with CellTracker green CMFDA (12.5 μM, Life Technologies, Milan, Italy). After three washes with blocking solution, cells were pre-incubated with increasing concentration of the compounds (10^{-10} – 10^{-4} M) or the vehicle (methanol) for 30 min at 37 °C. Next, cells were plated (500,000 cells/well) on FN or VCAM-1 coated wells, and the plate was incubated for 30 min at 37 °C. To remove non-adherent cells, wells were washed three times with blocking solution. Remaining adhered cells were lysed with 0.5 % Triton X-100 in PBS (Phosphate-buffered Saline, Life Technologies) for 30 min at 4 °C. Green fluorescence was measured (Ex485 nm/Em535 nm) using an EnSpire Multimode Plate Reader (PerkinElmer, Waltham, MA, USA).

Regarding adhesion assays on K562 and HL-60 cells, clear 96-well plates (Corning Costar) were coated overnight at 4 °C by passive adsorption with FN (10 μg/mL) or Fg (fibrinogen, 10 μg/mL) respectively. For adhesion assays mediated by $\alpha_5\beta_1$ integrin, K562 cells were treated with 64.85 nM PMA for 48 h to enhance $\alpha_5\beta_1$ integrin expression. On the day of the assay, plates were blocked with blocking solution (1 % BSA in PBS for K562 cells; 1 % BSA in HBSS for HL-60 cells) at 37 °C for

1 h; 30 min for HL-60 cells. Cells were then pre-incubated with increasing concentrations of the compounds (10^{-10} – 10^{-4} M) or the vehicle (methanol) for 30 min at room temperature. Afterward, cells were plated (50,000 cells/well) on coated wells and the plate was incubated for 1 h at room temperature. To remove non-adherent cells, wells were washed three times with blocking solution. Then, 50 μL/well of hexosaminidase substrate [1:1 solution of 4-nitrophenyl-N-acetyl-β-D-glucosaminide 7.5 mM in 0.09 M citrate buffer (pH 5.0) and 0.5 % Triton X-100 in H_2O] was added and incubated for 1 h at room temperature. Absorbance was measured at 405 nm after the addition of stopping solution (Glycine 50 mM; EDTA 5 mM; pH 10.4) using an EnSpire Multimode Plate Reader (PerkinElmer, Waltham, MA, USA).

The number of adherent cells was determined via comparison with a standard curve made in the same plate. Experiments were carried out in quadruplicate and repeated at least three times. Data analysis and EC_{50} (for agonists) or IC_{50} (for antagonists) were calculated using GraphPad Prism 10.4.1 (GraphPad Software, San Diego, CA, USA).

4.2.4. Western blot analysis

Western blot analysis was carried out as previously reported [38,59], with the following modifications. Jurkat E6.1 cells were serum-starved for 18 h in RPMI medium containing 1 % FBS. Then, 4×10^6 cells/-sample were treated with increasing concentrations (10^{-9}, 10^{-8}, 10^{-7} M) of the most potent $\alpha_4\beta_1$ integrin ligands for 1 h at 37 °C. Cells treated with $\alpha_4\beta_1$ integrin antagonists were subsequently incubated with FN (10 μg/mL) for 30 min at 37 °C. Cells treated with agonists were not incubated with fibronectin. Then, cells were lysed for 10 min at 4 °C by gently shaking using T-PER® (Tissue Protein Extraction Reagent, Life Technologies) added with a protease-phosphatase inhibitor cocktail (aprotinin 2 μg/mL; benzamidine 0.5 mg/mL; leupeptin 2 μg/mL; phenylmethylsulfonyl fluoride 2 mM; phosphatase inhibitor cocktail 1x). Cell debris were removed by centrifugation (12,000 g for 15 min at 4 °C) and protein concentration was determined using BCA Protein Assay kit (Thermo Scientific™ Pierce™, Rockford, IL, USA). Protein extracts were denatured at 95 °C for 3 min, then equal amounts of protein samples (30–70 μg) were loaded and separated via 12 % SDS-PAGE. Proteins were transferred onto a nitrocellulose membrane (Bio-Rad Laboratories S. r.l., Segrate, Milan), which was blocked for 1 h at room temperature with 5 % non-fat milk in a Tris-buffered saline (20 mM Tris-HCl; 0.25 mM 2-amino-2-(hydroxymethyl)-1,3-propanediol; 150 mM NaCl; pH 7.2) containing 0.1 % Tween-20. Membranes were stained overnight at 4 °C with anti-actin antibody (1:5000, Merck Life Science, Milan, Italy) or with anti-phospho-ERK1/2, anti-total-ERK1/2, anti-phospho-Akt, anti-total-Akt, or anti-phospho-JNK antibodies (all diluted 1:1000; Cell Signaling Technology, Danvers, MA, USA). The following day, membranes were washed 3 times with TBS-T 0.1 % and then incubated with peroxidase-conjugated secondary antibodies for 1.5 h under shaking at room temperature (1:8000; Santa Cruz Biotechnology). Blots were developed with chemiluminescent substrate (Clarity Western ECL Substrate) according to manufacturer's protocol (Bio-Rad Laboratories S. r.l., Segrate, Milan). Blot images were digitally acquired by ChemiDoc (Bio-Rad Laboratories S. r.l., Segrate, Milan, Italy). Protein expression was quantitatively analysed using Image Lab Software v.6.1 (Bio-Rad Laboratories S. r.l., Segrate, Milan, Italy). Experiments were replicated independently at least four times.

To assess the functional selectivity of the most promising new compounds towards a specific intracellular signaling pathway, we calculated the Pathway Selectivity Index (PSI) as the ratio between the areas under the curve (AUC) values of concentration-response curve of two kinases, specifically:

$$PSI = \frac{AUC_i}{AUC_k}$$

where i and k are the two kinases.

For $\alpha_4\beta_1$ integrin antagonists, values were interpreted as follows:

- PSI $\geq$1.5: Strong preference for "k" antagonism
- 1.33 $\leq$ PSI <1.5: Moderate preference for "k" antagonism
- 0.67 < PSI <1.33: No significant pathway preference
- 0.5 $\leq$ PSI $\leq$0.67: Moderate preference for "i" antagonism
- PSI <0.5: Strong preference for "i" antagonism

For $\alpha_4\beta_1$ integrin agonists, values were interpreted as follows:

- PSI $\geq$1.5: Strong preference for "i" agonism
- 1.33 $\leq$ PSI <1.5: Moderate preference for "i" agonism
- 0.67 < PSI <1.33: No significant pathway preference
- 0.5 $\leq$ PSI $\leq$0.67: Moderate preference for "k" agonism
- PSI <0.5: Strong preference for "k" agonism

This classification enables comparison of compounds' functional selectivity based on differential activation or inhibition of three signaling pathways.

CRediT authorship contribution statement

Valentina Giraldi: Writing – review & editing, Methodology, Investigation, Formal analysis, Data curation. **Andrea Maurizio:** Methodology, Investigation, Data curation. **Martina Cirillo:** Investigation, Data curation. **Paolo Magnone:** Data curation. **Emanuela Fedele:** Data curation. **Andrea Bedini:** Methodology. **Monica Baiula:** Writing – review & editing, Writing – original draft, Methodology, Funding acquisition, Data curation, Conceptualization. **Daria Giacomini:** Writing – review & editing, Writing – original draft, Supervision, Funding acquisition, Conceptualization.

Funding

This work was supported by the University of Bologna RFO 2023–24 and by The Project "Synthesis and biomedical applications of tumor targeting peptidomimetics and conjugates" by Ministero dell'Istruzione, dell'Università e della Ricerca (MIUR, PRIN2020), funding number 2020833Y75.

Declaration of competing interest

The authors declare that they have no known competing financial interests or personal relationships that could have appeared to influence the work reported in this paper.

Acknowledgements

DG and VG would acknowledge Roberto Cardinali and Giada Ombroso for technical assistance.

Appendix A. Supplementary data

Supplementary data to this article can be found online at https://doi.org/10.1016/j.ejmech.2025.117965.

Data availability

No data was used for the research described in the article.

References

[1] R.O. Hynes, Integrins: bidirectional, allosteric signaling machines, Cell 110 (2002) 673–687, https://doi.org/10.1016/s0092-8674(02)00971-6.
[2] Y. Takada, X. Ye, S. Simon, The integrins, Genome Biol. 8 (2007) 215, https://doi.org/10.1186/gb-2007-8-5-215.
[3] J.Z. Kechagia, J. Ivaska, P. Roca-Cusachs, Integrins as biomechanical sensors of the microenvironment, Nat. Rev. Mol. Cell Biol. 20 (2019) 457–473, https://doi.org/10.1038/s41580-019-0134-2.

[4] B.H. Luo, C.V. Carman, T.A. Springer, Structural basis of integrin regulation and signaling, Annu. Rev. Immunol. 25 (2007) 619–647, https://doi.org/10.1146/annurev.immunol.25.022106.141618.

[5] S. Seetharaman, S. Etienne-Manneville, Integrin diversity brings specificity in mechanotransduction, Biol. Cell 110 (2018) 49–64, https://doi.org/10.1111/boc.201700060.

[6] Z. Sun, S.S. Guo, R. Fassler, Integrin-mediated mechanotransduction, J. Cell Biol. 215 (2016) 445–456, https://doi.org/10.1083/jcb.2016090371.

[7] Y. Su, W. Xia, J. Li, T. Walz, M.J. Humphries, D. Vestweber, C. Cabañas, C. Lu, T. A. Springer, Relating conformation to function in integrin $\alpha_5\beta_1$, Proc. Natl. Acad. Sci. USA 113 (2016) E3872–E3881, https://doi.org/10.1073/pnas.1605074113.

[8] C. Yunfeng, L. Zhenhai, K. Fang, A.J. Lining, Z. Cheng, Force-regulated spontaneous conformational changes of integrins $\alpha_5\beta_1$ and $\alpha_V\beta_3$, ACS Nano 18 (2024) 299–313, https://doi.org/10.1021/acsnano.3c06253.

[9] Z. Li, A molecular arm: the molecular bending–unbending mechanism of integrin, Biomech. Model. Mechanobiol. 23 (2024) 781–792, https://doi.org/10.1007/s10237-023-01805-3.

[10] M. Barczyk, S. Carracedo, D. Gullberg, Integrins, Cell Tissue Res. 339 (2010) 269–280, https://doi.org/10.1007/s00441-009-0834-6.

[11] I.D. Campbell, M.J. Humphries, Integrin structure, activation, and interactions, Cold Spring Harbor Perspect. Biol. 3 (2011) a004994, https://doi.org/10.1101/cshperspect.a004994.

[12] Q. Zhang, S. Zhang, J. Chen, Z. Xie, The interplay between integrins and immune cells as a regulator in cancer immunology, Int. J. Mol. Sci. 24 (2023) 6170, https://doi.org/10.3390/ijms24076170.

[13] T. Klaus, C. Hieber, M. Bros, S. Grabbe, Integrins in health and disease, suitable targets for treatment? Cells 13 (2024) 212, https://doi.org/10.3390/cells13030212.

[14] X. Pang, X. He, Z. Qiu, H. Zhang, R. Xie, Z. Liu, Y. Gu, N. Zhao, Q. Xiang, Y. Cui, Targeting integrin pathways: mechanisms and advances in therapy, Signal Transduct. Targeted Ther. 8 (2023) 1, https://doi.org/10.1038/s41392-022-01259-6.

[15] C.L. Abram, C.A. Lowell, The ins and outs of leukocyte integrin signaling, Annu. Rev. Immunol. 27 (2009) 339–362, https://doi.org/10.1146/annurev.immunol.021908.132554.

[16] R. Sumagin, H. Prizant, E. Lomakina, R.E. Waugh, I.H. Sarelius, LFA-1 and Mac-1 define characteristically different intralumenal crawling and emigration patterns for monocytes and neutrophils in situ, J. Immunol. 49 (2010) 1841–1850, https://doi.org/10.4049/jimmunol.1001638.

[17] Y.M. Hyun, Y.H. Choe, S.A. Park, M. Kim, LFA-1 (CD11a/CD18) and Mac-1 (CD11b/CD18) distinctly regulate neutrophil extravasation through hotspots I and II, Exp. Mol. Med. 51 (2019) 1–13, https://doi.org/10.1038/s12276-019-0227-1.

[18] H.E. Conley, M.K. Sheats, Targeting neutrophil β_2-integrins: a review of relevant resources, tools, and methods, Biomolecules 13 (2023) 892, https://doi.org/10.3390/biom13060892.

[19] P. Bouti, B.J.A.M. Klein, P.J.H. Verkuijlen, K. Schornagel, F.P.J. van Alphen, K. H. Taris, M. van den Biggelaar, A.J. Hoogendijk, R. van Bruggen, T.W. Kuijpers, H. L. Matlung, SKAP2 acts downstream of CD11b/CD18 and regulates neutrophil effector function, Front. Immunol. 15 (2024) 1344761, https://doi.org/10.3389/fimmu.2024.1344761.

[20] K. Yonekawa, J.M. Harlan, Targeting leukocyte integrins in human diseases, J. Leukoc. Biol. 77 (2005) 129–140, https://doi.org/10.1189/jlb.0804460.

[21] I. Mitroulis, V.I. Alexaki, I. Kourtzelis, A. Ziogas, G. Hajishengallis, T. Chavakis, Leukocyte integrins: role in leukocyte recruitment and as therapeutic targets in inflammatory disease, Pharmacol. Ther. 147 (2015) 123–135, https://doi.org/10.1016/j.pharmthera.2014.11.008.

[22] L. Schittenhelm, C.M. Hilkens, V.L. Morrison, β_2 Integrins as regulators of dendritic cell, monocyte, and macrophage function, Front. Immunol. 8 (2017) 1866, https://doi.org/10.3389/fimmu.2017.01866.

[23] A.J. Kelly, A. Long, Targeting T-cell integrins in autoimmune and inflammatory diseases, Clin. Exp. Immunol. 215 (2024) 15–26, https://doi.org/10.1093/cei/uxad093.

[24] K. Ławkowska, K. Bonowicz, D. Jerka, Y. Bai, M. Gagat, Integrins in cardiovascular health and disease: molecular mechanisms and therapeutic opportunities, Biomolecules 15 (2025) 233, https://doi.org/10.3390/biom15020233.

[25] C. Su, J. Mo, S. Dong, Z. Liao, B. Zhang, P. Zhu, Integrin β-1 in disorders and cancers: molecular mechanisms and therapeutic targets, Cell Commun. Signal. 22 (2024) 71, https://doi.org/10.1186/s12964-023-01338-3.

[26] M.C. Bellavia, L. Nyiranshuti, J.D. Latoche, K.V. Ho, R.J. Fecek, J.L. Taylor, K. E. Day, S. Nigam, M. Pun, F. Gallazzi, R.S. Edinger, W.J. Storkus, R.B. Patel, C. J. Anderson, PET imaging of VLA-4 in a new BRAFV600E mouse model of melanoma, Mol. Imag. Biol. 24 (2022) 425–433, https://doi.org/10.1007/s11307-021-01666-1.

[27] A. Hickman, J. Koetsier, T. Kurtanich, M.C. Nielsen, G. Winn, Y. Wang, S. E. Bentebibel, L. Shi, S. Punt, L. Williams, C. Haymaker, C.B. Chesson, F. Fa'ak, A. L. Dominguez, R. Jones, I. Kuiatse, A.R. Caivano, S. Khounlo, N.D. Warier, U. Marathi, R.V. Market, R.J. Biediger, J.W. Craft Jr., P. Hwu, M.A. Davies, D. G. Woodside, P. Vanderslice, A. Diab, W.W. Overwijk, Y. Hailemichael, LFA-1 activation enriches tumor-specific T cells in a cold tumor model and synergizes with CTLA-4 blockade, J. Clin. Investig. 132 (2022) e154152, https://doi.org/10.1172/JCI154152.

[28] M. Baiula, S. Spampinato, L. Gentilucci, A. Tolomelli, Novel ligands targeting $\alpha_4\beta_1$ integrin: therapeutic applications and perspectives, Front. Chem. 7 (2019) 489, https://doi.org/10.3389/fchem.2019.00489.

[29] T. He, D. Giacomini, A. Tolomelli, M. Baiula, L. Gentilucci, Conjecturing about small-molecule agonists and antagonists of $\alpha_4\beta_1$ integrin: from mechanistic insight to potential therapeutic applications, Biomedicines 12 (2024) 316, https://doi.org/10.3390/biomedicines12020316.

[30] B. LaFoya, J.A. Munroe, A. Miyamoto, M.A. Detweiler, J.J. Crow, T. Gazdik, A. R. Albig, Beyond the matrix: the many non-ECM ligands for integrins, Int. J. Mol. Sci. 19 (2018) 449, https://doi.org/10.3390/ijms19020449.

[31] N. Nishida, C. Xie, M. Shimaoka, Y. Cheng, T. Walz, T.A. Springer, Activation of leukocyte beta2 integrins by conversion from bent to extended conformations, Immunity 25 (2006) 583–594, https://doi.org/10.1016/j.immuni.2006.07.016.

[32] Y. Zheng, K. Leftheris, Insights into protein-ligand interactions in integrin complexes: advances in structure determinations, J. Med. Chem. 63 (2020) 5675–5696, https://doi.org/10.1021/acs.jmedchem.9b01869.

[33] E.F. Plow, T.A. Haas, L. Zhang, J. Loftus, J.W. Smith, Ligand binding to integrins, J. Biol. Chem. 275 (2000) 21785–21788, https://doi.org/10.1074/jbc.R000003200.

[34] V.H. Tselepis, L.J. Green, M.J. Humphries, An RGD to LDV motif conversion within the disintegrin kistrin generates an integrin antagonist that retains potency but exhibits altered receptor specificity. Evidence for a functional equivalence of acidic integrin-binding motifs, J. Biol. Chem. 272 (1997) 21341–21348, https://doi.org/10.1074/jbc.272.34.21341.

[35] J.L. Viney, S. Jones, H.H. Chiu, B. Lagrimas, M.E. Renz, L.G. Presta, D. Jackson, K. J. Hillan, S. Lew, S. Fong, Mucosal addressing cell adhesion molecule-1: a structural and functional analysis demarcates the integrin binding motif, J. Immunol. 157 (1996) 2488–2497, https://doi.org/10.4049/jimmunol.157.6.2488.

[36] T. Getter, R. Margalit, S. Kahremany, L. Levy, E. Blum, N. Khazanov, N.Y. Keshet-Levy, T.Y. Tamir, M. Ben Major, R. Lahav, S. Zilber, H. Senderowitz, P. Bradfield, B. A. Imhof, E. Alpert, A. Gruzman, Novel inhibitors of leukocyte transendothelial migration, Bioorg. Chem. 92 (2019) 103250, https://doi.org/10.1016/j.bioorg.2019.103250.

[37] D. Gottschling, J. Boer, A. Schuster, B. Holzmann, H. Kessler, Combinatorial and rational strategies to develop nonpeptidic alpha4beta7-integrin antagonists from cyclic peptides, Angew Chem. Int. Ed. Engl. 41 (2002) 3007–3011, https://doi.org/10.1002/1521-3773(20020816)41:16<3007::AID-ANIE3007>3.0.CO;2-3.

[38] J.P. Wu, J. Emeigh, D.A. Gao, D.R. Goldberg, D. Kuzmich, C. Miao, I. Potocki, K. C. Qian, R.J. Sorcek, D.D. Jeanfavre, K. Kishimoto, E.A. Mainolfi, G. Nabozny Jr., C. Peng, P. Reilly, R. Rothlein, R.H. Sellati, J.R. Woska Jr., S. Chen, J.A. Gunn, D. O'Brien, S.H. Norris, T.A. Kelly, Second-generation lymphocyte function-associated antigen-1 inhibitors: 1H-imidazo[1,2-alpha]imidazole-2-one derivatives, J. Med. Chem. 47 (2004) 5356–5366, https://doi.org/10.1021/jm049657b.

[39] D. Cox, M. Brennan, N. Moran, Integrins as therapeutic targets: lessons and opportunities, Nat. Rev. Drug Discov. 9 (2010) 804–820, https://doi.org/10.1038/nrd3266. PMID: 20885411.

[40] K. Ley, J. Rivera-Nieves, W.J. Sandborn, S. Shattil, Integrin-based therapeutics: biological basis, clinical use and new drugs, Nat. Rev. Drug Discov. 15 (2016) 173–183, https://doi.org/10.1038/nrd.2015.10.

[41] K. Matsuoka, M. Watanabe, T. Ohmori, K. Nakajima, T. Ishida, Y. Ishiguro, K. Kanke, K. Kobayashi, F. Hirai, K. Watanabe, H. Mizusawa, S. Kishida, Y. Miura, A. Ohta, T. Kajioka, T. Hibi, AJM300 Study Group, AJM300 (carotegrast methyl), an oral antagonist of α4-integrin, as induction therapy for patients with moderately active ulcerative colitis: a multicentre, randomised, double-blind, placebo-controlled, phase 3 study, Lancet Gastroenterol, Hepatology 7 (2022) 648–657, https://doi.org/10.1016/S2468-1253(22)00022-X.

[42] M. Baiula, P. Galletti, G. Martelli, R. Soldati, L. Belvisi, M. Civera, S.D. Dattoli, S. M. Spampinato, D. Giacomini, New β-lactam derivatives modulate cell adhesion and signaling mediated by RGD-binding and leukocyte integrins, J. Med. Chem. 59 (2016) 9721–9742, https://doi.org/10.1021/acs.jmedchem.6b00576.

[43] G. Martelli, M. Baiula, A. Caligiana, P. Galletti, L. Gentilucci, R. Artali, S. Spampinato, D. Giacomini, Could dissecting the molecular framework of β-lactam integrin ligands enhance selectivity? J. Med. Chem. 62 (2019) 10156–10166, https://doi.org/10.1021/acs.jmedchem.9b01000.

[44] R.Z. Panni, J.M. Herndon, C. Zuo, S. Hegde, G.D. Hogg, B.L. Knolhoff, M.A. Breden, X. Li, V.E. Krisnawan, S.Q. Khan, J.K. Schwarz, B.E. Rogers, R.C. Fields, W. G. Hawkins, V. Gupta, D.G. DeNardo, Agonism of CD11b reprograms innate immunity to sensitize pancreatic cancer to immunotherapies, Sci. Transl. Med. 11 (2019) eaau9240, https://doi.org/10.1126/scitranslmed.aau9240.

[45] X. Liu, G.D. Hogg, C. Zuo, N.C. Borcherding, J.M. Baer, V.E. Lander, L.I. Kang, B. L. Knolhoff, F. Ahmad, R.E. Osterhout, A.V. Galkin, J.M. Bruey, L.L. Carter, C. Mpoy, K.R. Vij, R.C. Fields, J.K. Schwarz, H. Park, V. Gupta, D.G. DeNardo, Context-dependent activation of STING-interferon signaling by CD11b agonists enhances anti-tumor immunity, Cancer Cell 41 (2023) 1073–1090.e12, https://doi.org/10.1016/j.ccell.2023.04.018.

[46] G. Martelli, N. Bloise, A. Merlettini, G. Bruni, L. Visai, M.L. Focarete, D. Giacomini, Combining biologically active β-lactams integrin agonists with poly(l-lactic acid) nanofibers: enhancement of human mesenchymal stem cell adhesion, Biomacromolecules 21 (2020) 1157–1170, https://doi.org/10.1021/acs.biomac.9b01550.

[47] M. Cirillo, G. Martelli, E. Boanini, K. Rubini, M. Di Filippo, P. Torricelli, S. Pagani, M. Fini, A. Bigi, D. Giacomini, Strontium substituted hydroxyapatite with β-lactam integrin agonists to enhance mesenchymal cells adhesion and to promote bone regeneration, Colloids Surf. B Biointerfaces 200 (2021) 111580, https://doi.org/10.1016/j.colsurfb.2021.111580.

[48] V.A. Baldassarro, V. Giraldi, A. Giuliani, M. Moretti, G. Pagnotta, A. Flagelli, P. Clavenzani, L. Lorenzini, L. Giardino, M.L. Focarete, D. Giacomini, L. Calzà, Poly (l-lactic acid) scaffold releasing an $\alpha_4\beta_1$ integrin agonist promotes nonfibrotic skin

wound healing in diabetic mice, ACS Appl. Bio Mater. 16 (2023) 296–308, https://doi.org/10.1021/acsabm.2c00890.
[49] M. Anselmi, M. Baiula, S. Spampinato, R. Artali, T. He, L. Gentilucci, Design and pharmacological characterization of $\alpha_4\beta_1$ integrin cyclopeptide agonists: computational investigation of ligand determinants for agonism versus antagonism, J. Med. Chem. 66 (2023) 5021–5040, https://doi.org/10.1021/acs.jmedchem.2c02098.
[50] E.P. Gillis, K.J. Eastman, M.D. Hill, D.J. Donnelly, N.A. Meanwell, Applications of fluorine in medicinal chemistry, J. Med. Chem. 58 (2015) 8315–8359, https://doi.org/10.1021/acs.jmedchem.5b00258.
[51] S. Purser, P.R. Moore, S. Swallow, V. Gouverneur, Fluorine in medicinal chemistry, Chem. Soc. Rev. 37 (2008) 320–330, https://doi.org/10.1039/b610213c.
[52] J.D. Humphries, J.A. Askari, X.P. Zhang, Y. Takada, M.J. Humphries, A.P. Mould, Molecular basis of ligand recognition by integrin alpha$_5$beta$_1$. II. Specificity of Arg-Gly-Asp binding is determined by Trp157 of the alpha subunit, J. Biol. Chem. 275 (2000) 20337–20345, https://doi.org/10.1074/jbc.M000568200.
[53] W. Xia, T.A. Springer, Metal ion and ligand binding of integrin $\alpha_5\beta_1$, Proc. Natl. Acad. Sci. U. S. A 111 (2014) 17863–17868, https://doi.org/10.1073/pnas.1420645111.
[54] J.M. Anderson, J. Li, T.A. Springer, Regulation of integrin $\alpha_5\beta_1$ conformational states and intrinsic affinities by metal ions and the ADMIDAS, Mol. Biol. Cell 33 (2022) ar56, https://doi.org/10.1091/mbc.E21-11-0536.
[55] J. Li, Y. Su, W. Xia, Y. Qin, M.J. Humphries, D. Vestweber, C. Cabañas, C. Lu, T. A. Springer, Conformational equilibria and intrinsic affinities define integrin activation, EMBO J. 36 (2017) 629–645, https://doi.org/10.15252/embj.201695803.
[56] F.Y. Lin, J. Li, Y. Xie, J. Zhu, T.T. Huong Nguyen, Y. Zhang, J. Zhu, T.A. Springer, A general chemical principle for creating closure-stabilizing integrin inhibitors, Cell 185 (2022) 3533–3550 e27, https://doi.org/10.1016/j.cell.2022.08.008.
[57] D.N. Edwards, K. Salmeron, D.E. Lukins, A.L. Trout, J.F. Fraser, G.J. Bix, Integrin $\alpha_5\beta_1$ inhibition by ATN-161 reduces neuroinflammation and is neuroprotective in ischemic stroke, J. Cerebr. Blood Flow Metabol. 40 (2020) 1695–1708, https://doi.org/10.1177/0271678X19880161.
[58] C. Lamers, C.J. Plüss, D. Ricklin, The promiscuous profile of complement receptor 3 in ligand binding, immune modulation, and pathophysiology, Front. Immunol. 12 (2021) 662164, https://doi.org/10.3389/fimmu.2021.662164.
[59] H. Nguyen, N.P. Podolnikova, T.P. Ugarova, X. Wang, α_MI-domain of integrin Mac-1 binds the cytokine pleiotrophin using multiple mechanisms, Structure 32 (2024) 1184–1196, https://doi.org/10.1016/j.str.2024.04.013, e4.
[60] N.P. Podolnikova, A.V. Podolnikov, T.A. Haas, V.K. Lishko, T.P. Ugarova, Ligand recognition specificity of leukocyte integrin $\alpha_M\beta_2$ (Mac-1, CD11b/CD18) and its functional consequences, Biochemistry 54 (2015) 1408–1420, https://doi.org/10.1021/bi5013782.
[61] D. Maiguel, M.H. Faridi, C. Wei, Y. Kuwano, K.M. Balla, D. Hernandez, C.J. Barth, G. Lugo, M. Donnelly, A. Nayer, L.F. Moita, S. Schürer, D. Traver, P. Ruiz, R. I. Vazquez-Padron, K. Ley, J. Reiser, V. Gupta, Small molecule-mediated activation of the integrin CD11b/CD18 reduces inflammatory disease, Sci. Signal. 4 (2011) ra57, https://doi.org/10.1126/scisignal.2001811.
[62] R. Nussinov, M. Zhang, Y. Liu, H. Jang, AlphaFold, allosteric, and orthosteric drug discovery: ways forward, Drug Discov. Today 28 (2023) 103551, https://doi.org/10.1016/j.drudis.2023.103551.
[63] D.G. DeNardo, A. Galkin, J. Dupont, L. Zhou, J. Bendell, GB1275, a first-in-class CD11b modulator: rationale for immunotherapeutic combinations in solid tumors, J. Immunother. Cancer 9 (2021) e003005, https://doi.org/10.1136/jitc-2021-003005.
[64] P. Bouti, S.D.S. Webbers, S.C. Fagerholm, R. Alon, M. Moser, H.L. Matlung, T. W. Kuijpers, β_2 Integrin signaling cascade in neutrophils: more than a single function, Front. Immunol. 11 (2021) 619925, https://doi.org/10.3389/fimmu.2020.619925.
[65] T. Geraghty, A. Rajagopalan, R. Aslam, A. Pohlman, I. Venkatesh, A. Zloza, D. Cimbaluk, D.G. DeNardo, V. Gupta, Positive allosteric modulation of CD11b as a novel therapeutic strategy against lung cancer, Front. Oncol. 10 (2020) 748, https://doi.org/10.3389/fonc.2020.00748.
[66] P.G. Ruminski, M.P. Rettig, J.F. DiPersio, Development of VLA4 and CXCR4 antagonists for the mobilization of hematopoietic stem and progenitor cells, Biomolecules 14 (2024) 1003, https://doi.org/10.3390/biom14081003.
[67] T. He, D. Giacomini, A. Tolomelli, M. Baiula, L. Gentilucci, Conjecturing about small-molecule agonists and antagonists of $\alpha_4\beta_1$ integrin: from mechanistic insight to potential therapeutic applications, Biomedicines 12 (2024) 316, https://doi.org/10.3390/biomedicines12020316.
[68] M. Merdanovic, S.G. Burston, A.L. Schmitz, M. Ehrmann, Activation by substoichiometric inhibition, Proc. Natl. Acad. Sci. USA 117 (2020) 1414–1418, https://doi.org/10.1073/pnas.1918721117.
[69] U. Reuning, V.M. D'Amore, K. Hodivala-Dilke, L. Marinelli, H. Kessler, Importance of integrin transmembrane helical interactions for antagonistic versus agonistic ligand behavior: consequences for medical applications, Bioorg. Chem. 156 (2025) 108193, https://doi.org/10.1016/j.bioorg.2025.108193.
[70] W. Yang, C.V. Carman, M. Kim, A. Salas, M. Shimaoka, T.A. Springer, A small molecule agonist of an integrin, $\alpha_L\beta_2$, J. Biol. Chem. 281 (2006) 37904–37912, https://doi.org/10.1074/jbc.M606888200.
[71] F.Y. Lin, J. Zhu, E.T. Eng, N.E. Hudson, T.A. Springer, β-Subunit binding is sufficient for ligands to open the integrin $\alpha_{IIb}\beta_3$ headpiece, J. Biol. Chem. 291 (9) (2016 Feb 26) 4537–4546, https://doi.org/10.1074/jbc.M115.705624. Epub 2015 Dec 2. PMID: 26631735; PMCID: PMC4813479.
[72] P. Kanchanawong, D.A. Calderwood, Organization, dynamics and mechanoregulation of integrin-mediated cell-ECM adhesions, Nat. Rev. Mol. Cell Biol. 24 (2023) 142–161, https://doi.org/10.1038/s41580-022-00531-5.
[73] D.I. Simon, Opening the field of integrin biology to "biased agonism", Circ. Res. 109 (2011) 1199–1201, https://doi.org/10.1161/CIRCRESAHA.111.257980.
[74] A. Tolomelli, P. Galletti, M. Baiula, D. Giacomini, Can integrin agonists have cards to play against cancer? A literature survey of small molecules integrin activators, Cancers 9 (2017) 78, https://doi.org/10.3390/cancers9070078.
[75] Y.K. Takada, M. Shimoda, Y. Takada, CD40L activates platelet integrin $\alpha_{IIb\beta3}$ by binding to the allosteric site (site 2) in a KGD-independent manner and HIGM1 mutations are clustered in the integrin-binding sites of CD40L, Cells 12 (2023) 1977, https://doi.org/10.3390/cells12151977.
[76] R.V. Mancuso, G. Schneider, M. Hürzeler, M. Gut, J. Zurflüh, W. Breitenstein, J. Bouitbir, F. Reisen, K. Atz, C. Ehrhardt, U. Duthaler, D. Gygax, A.G. Schmidt, S. Krähenbühl, G. Weitz-Schmidt, Allosteric targeting resolves limitations of earlier LFA-1 directed modalities, Biochem. Pharmacol. 211 (2023) 115504, https://doi.org/10.1016/j.bcp.2023.115504.
[77] Y.K. Takada, M. Shimoda, E. Maverakis, B.H. Felding, R.H. Cheng, Y. Takada, Soluble CD40L activates soluble and cell-surface integrin $\alpha_v\beta_3$, $\alpha_5\beta_1$, and $\alpha_4\beta_1$ by binding to the allosteric ligand-binding site (site 2), J. Biol. Chem. 296 (2021) 100399, https://doi.org/10.1016/j.jbc.2021.100399.
[78] Y. Huang, P.S. Hammond, B.R. Whirrett, R.J. Kuhner, L. Wu, S.R. Childers, R. H. Mach, Synthesis and quantitative structure−activity relationships of *N*-(1-benzylpiperidin-4-yl)phenylacetamides and related analogues as potent and selective σ1 receptor ligands, J. Med. Chem. 41 (1998) 2361–2370, https://doi.org/10.1021/jm980032l.
[79] I. Bae, D. Kim, J. Choi, J. Kim, M. Kim, B. Park, Y.H. Kim, Y.G. Ahn, H.H. Kim, D. K. Kim, Design, synthesis and biological evaluation of new bivalent quinazoline analogues as IAP antagonists, Bioorg. Med. Chem. Lett. 34 (2021) 127676, https://doi.org/10.1016/j.bmcl.2020.127676.
[80] T.M. Bräuer, Q. Zhang, K. Tiefenbacher, Iminium catalysis inside a self-assembled supramolecular capsule: modulation of enantiomeric excess, Angew. Chem. Int. Ed. 55 (2016) 7698–7701, https://doi.org/10.1002/anie.201602382.
[81] P. Galletti, R. Soldati, M. Pori, M. Durso, A. Tolomelli, L. Gentilucci, S.D. Dattoli, M. Baiula, S. Spampinato, D. Giacomini, Targeting integrins $\alpha_v\beta_3$ and $\alpha_5\beta_1$ with new β-lactam derivatives, Eur. J. Med. Chem. 83 (2014) 284–293, https://doi.org/10.1016/j.ejmech.2014.06.041.
[82] J. Lee, M.-K. Jin, S.-U. Kang, S.Y. Kim, J. Lee, M. Shin, J. Hwang, S. Cho, Y.-S. Choi, H.-K. Choi, S.-E. Kim, Y.-G. Suh, Y.-S. Lee, Y.-H. Kim, H.-J. Ha, A. Toth, L.V. Pearce, R. Tran, T. Szabo, J.D. Welter, D.J. Lundberg, Y. Wang, J. Lazar, V.A. Pavlyukovets, M.A. Morgan, P.M. Blumberg, Analysis of structure–activity relationships for the 'B-region' of N-(4-t-butylbenzyl)-N′-[4-(methyl sulfonylamino) benzyl]-thiourea analogues as TRPV1 antagonists, Bioorg. Med. Chem. Lett. 15 (2005) 4143–4150, https://doi.org/10.1016/j.bmcl.2005.06.009.
[83] V. Perron, S. Abbott, N. Moreau, D. Lee, C. Penney, B. Zacharie, A Method for the selective protection of aromatic amines in the presence of aliphatic amines, Synthesis 2 (2009) 283–289, https://doi.org/10.1055/s-0028-1083290.
[84] C. Bolchi, E. Valoti, L. Fumagalli, V. Straniero, P. Ruggeri, M. Pallavicini, Enantiomerically pure dibenzyl esters of l-Aspartic and l-Glutamic acid, Org. Process Res. Dev. 19 (2015) 878–883, https://doi.org/10.1021/acs.oprd.5b00134.
[85] R.J. Tokarski, C.M. Sharp, A.C. Huntsman, B.K. Mize, O.R. Ayinde, E.H. Stahl, J. R. Lerma, A. Reed, B. Carmichael, N. Muthusamy, J.C. Byrd, J.R. Fuchs, Bifunctional degraders of cyclin dependent kinase 9 (CDK9): probing the relationship between linker length, properties, and selective protein degradation, Eur. J. Med. Chem. 254 (2023) 115342, https://doi.org/10.1016/j.ejmech.2023.115342.
[86] S.D. Dattoli, M. Baiula, R. De Marco, A. Bedini, M. Anselmi, L. Gentilucci, S. Spampinato, DS-70, a novel and potent α_4 integrin antagonist, is an effective treatment for experimental allergic conjunctivitis in Guinea pigs, Br. J. Pharmacol. 175 (2018) 3891–3910.
[87] M. Baiula, M. Anselmi, F. Musiani, A. Ghidini, J. Carbone, A. Caligiana, A. Maurizio, S. Spampinato, L. Gentilucci, Design, pharmacological characterization, and molecular docking of minimalist peptidomimetic antagonists of $\alpha_4\beta_1$ integrin, Int. J. Mol. Sci. 24 (2023) 9588, https://doi.org/10.3390/ijms24119588.
[88] M. Baiula, M. Cirillo, G. Martelli, V. Giraldi, E. Gasparini, A.C. Anelli, S. M. Spampinato, D. Giacomini, Selective integrin ligands promote cell internalization of the antineoplastic agent fluorouracil, ACS Pharmacol. Transl. Sci. 4 (2021) 1528–1542, https://doi.org/10.1021/acsptsci.1c00094.